journal of the international meteor organization

WGN

41:3
june 2013

New meteor showers
ν-Cygnids confirmed
Comet 17P/Holmes dust trail
NEMETODE overview and results
February–March video meteors

ISSN 1016-3115

WGN Vol. 41, No. 3, June 2013, pp. 69 – 100

Administrative

Meteor science

Ongoing meteor work

Preliminary results

Front cover photo

Composite image of the 2010 Perseid maximum, created from selected photographs containing meteors. Images were obtained on 2010 August 12/13 and 13/14, using Canon EOS 400D camera with 18 mm $f/2.8$ lens, set to ISO 1600 and 30 s exposures. Photo courtesy of Audrius Dubietis.

Writing for WGN This Journal welcomes papers submitted for publication. All papers are reviewed for scientific content, and edited for English and style. Instructions for authors can be found in WGN **31:4**, 124–128, and at `http://www.imo.net/docs/writingforwgn.pdf` .

Cover design Rainer Arlt

Legal address International Meteor Organization, Mattheessensstraat 60, 2540 Hove, Belgium.

Editorial

Javor Kac

The June *WGN* reaches you with a substantial delay. A long chain of events take place before *WGN* reaches our subscribers. After an article is submitted, a Handling Editor is assigned. He takes care of the manuscript content, checking both the scientific content and proper use of English. This often involves reviewers chosen from the *WGN* Editorial board, Advisory board, or other experts. When the content is ready and approved by both editor and authors, the editor may also take care of manuscript conversion to LaTeX code. Authors can ease editor's job by having their manuscript proofread for English, coding it in LaTeX, and making sure plots in figures are clearly legible and all figures are provided as separate files. The Editor-in-chief then takes over, preparing the final layout of the article. He assembles a series of articles into an issue body. The contents page and issue covers are then created. Producing the front cover involves another Editorial board member. The whole issue is then proofread once again for any possible errors introduced while it was assembled. Next, it is sent to Germany where it is printed and mailed. At the same time, the electronic version is uploaded to the IMO web pages and an announcement about its availability is sent out.

While there are some tasks in the *WGN* production process that are distributed and can be handled by many individuals, there are also some steps that involve only one person. We are working on strengthening the weaker links in the *WGN* production chain.

Despite the issue being somewhat late it brings some interesting topics. Two papers are related to discovery of new showers and confirmation of a listed meteor shower. An interesting opportunity to image the dust trail of the comet 17P/Holmes is presented in a paper that details successful observation of the dust trail in the past and provides its coordinates until the year 2015. Observers having access to big telescopes are invited to try imaging the phenomenon. Another paper announces a new video network in England. And as always, two monthly reports of the IMO Video Meteor Network are presented.

I hope you will enjoy reading this issue of *WGN* and forgive us the late delivery.

IMO bibcode WGN-413-editorial NASA-ADS bibcode 2013JIMO...41Q..69K

Call for photographs

Javor Kac

We are frequently short of photographs for the *WGN* covers that we publish in colour (front cover) or black&white (back cover). If you think you have a suitable meteor-related photograph, please offer it to us. More or less any computer image format will do. You can send your photographs to `wgn@imo.net`, but remember to put 'Meteor' in the subject line to get round the anti-spam filters.

IMO bibcode WGN-413-kac-call NASA-ADS bibcode 2013JIMO...41R..69K

Letter — The CMN catalogue of orbits for 2010

Croatian Meteor Network [1]

The Croatian Meteor Network (CMN) has released its catalogue of orbits for 2010. The catalogue contains 9436 orbits. It can be accessed from the CMN download page:
`http://cmn.rgn.hr/downloads/downloads.html`

[1] Email: `cmn@rgn.hr`

IMO bibcode WGN-413-cmn-letter NASA-ADS bibcode 2013JIMO...41L..69C

Meteor science

8 new showers from Croatian Meteor Network data

Damir Šegon [1], Željko Andreić [2], Korado Korlević [3], Filip Novoselnik [4], Denis Vida [5] and Ivica Skokić [6]

The Croatian Meteor Network Catalogues of Orbits for 2007 to 2010 contain 10 645 orbits of sporadic meteors. The radiant analysis that included all these orbits, plus the orbits from SonotaCo catalogues for 2007 to 2011, revealed 8 possible new streams. The streams were reported to the IAU MDC and got temporary IAU shower numbers and three-letter codes. We present the basic orbital, radiant and activity data for these streams.

Received 2012 October 31

1 Introduction

The Croatian Meteor Network (CMN) is in operation since 2007. The network itself is described in more detail in Andreić & Šegon (2010) and Andreić et al. (2010). The catalogues of orbits for 2007 to 2009 are already published (Šegon et al., 2012a; Korlević et al., 2013) and the catalogue for 2010 will be issued soon.

2 New showers

Radiant analysis of 133 653 orbits from CMN catalogues for 2007 to 2010 and SonotaCo catalogues from 2007 to 2011 (SonotaCo, 2012) resulted in 8 potential new showers that had not yet been reported to the IAU database. For each of these showers the individual orbits of meteoroids were selected with the D-criterion as in Šegon et al. (2012b), using the commonly employed Southworth-Hawkins method (Southworth & Hawkins, 1963; Jopek & Froeschlé, 1997). For each shower, a mean orbit was calculated from the individual orbits that satisfy $D_{SH} < 0.15$. The results of this analysis are summarized in Table 4. The file with all individual orbits of the new showers mentioned in this article can be downloaded from the CMN download page:

`http://cmn.rgn.hr/downloads/downloads.html`

It should be noted here that all these showers are present in the IMO Video Meteor Database (IMO, 2012). The showers were reported to the IAU, following the standard procedure (Jenniskens et al., 2009), and temporary shower numbers were obtained for them. Comet and near-Earth asteroid databases were also searched for possible parent bodies, with results listed below where appropriate.

2.1 κ Virginids – 509 KVI

This shower is active from March 3 to April 14. With 58 known orbits, we have enough data to see some interesting properties of this shower. The most obvious one is that the radiant seems to be spread over quite a large area of the sky (Figure 1). Similarly, the orbits are quite dispersed from the mean orbit of the shower. This could indicate an old shower or a shower composed of several filaments. This assumption is further supported by the long duration of the shower. However, the radiant plot clearly shows the effects of daily motion of the radiant, so the large spread of the radiant can be at least partially attributed to the daily motion. Due to the relatively large number of known orbits it is possible to determine the mean daily motion of the radiant: ΔRA $= 0.92°$/day, ΔDEC $= -0.35°$/day. Also, the radiant plot does not show any noticeable clustering that would indicate the existence of different filaments. But, for a more firm conclusion a lot more orbits are needed.

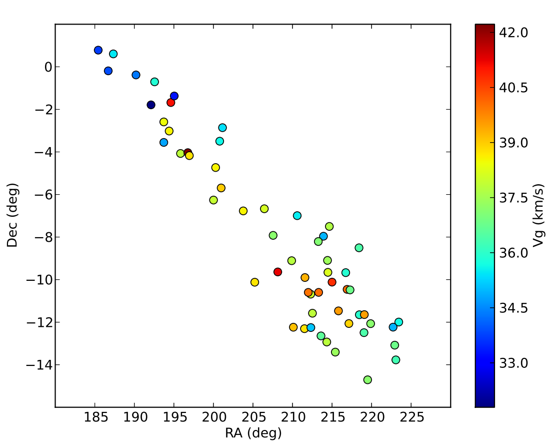

Figure 1 – Radiant plot of κ Virginids.

[1] Astronomical Society Istra Pula, Park Monte Zaro 2, 52100 Pula, Croatia.
Višnjan Science and Education Center, Istarska 5, 51463 Višnjan, Croatia.
Email: damir.segon@pu.htnet.hr

[2] University of Zagreb, Faculty of Mining, Geology and Petroleum Engineering, Pierottijeva 6, 10000 Zagreb, Croatia.
Email: zandreic@rgn.hr

[3] Višnjan Science and Education Center, Istarska 5, 51463 Višnjan, Croatia.
Email: korado@astro.hr

[4] Astronomical Society "Anonymus", B. Radića 34, 31550 Valpovo, Croatia and Faculty of Electrical Engineering, University of Osijek, Kneza Trpimira 2B, 31000 Osijek, Croatia.
Email: novoselnikf@gmail.com

[5] Astronomical Society "Anonymus", B. Radića 34, 31550 Valpovo, Croatia and Faculty of Electrical Engineering, University of Osijek, Kneza Trpimira 2B, 31000 Osijek, Croatia.
Email: denis.vida@gmail.com

[6] Astronomical Society "Anonymus", B. Radića 34, 31550 Valpovo, Croatia and Faculty of Electrical Engineering, University of Osijek, Kneza Trpimira 2B, 31000 Osijek, Croatia.
Email: ivica.skokic@gmail.com

IMO bibcode WGN-413-segon-8new
NASA-ADS bibcode 2013JIMO...41...70S

Table 1 – Comparison of orbital elements of κ Virginids (mean orbit) and the orbit of asteroid 2011 BT_{59}.

parameter	509 KVI	2011 BT_{59}
q	0.139	0.128
e	0.938	0.949
ω	321	303.0
Ω	6	39.0
i	8	3.6

The parent body search reveals asteroid 2011 BT_{59} as a weak match to the mean shower orbit, with $D_{SH} = 0.262$ (see Table 1).

2.2 June ρ Cygnids – 510 JRC

Contrary to the previous shower, the June ρ Cygnids have a very well defined radiant (Figure 2). The mean orbit is also well defined, regardless of the small number of known orbits (16). The shower is active from June 6 to June 20, the short activity period indicating a relatively young shower. The mean daily motion of the radiant is roughly ΔRA $\approx 0.4°$/day, ΔDEC $\approx 0.6°$/day, but due to the small number of known orbits these values are not accurate.

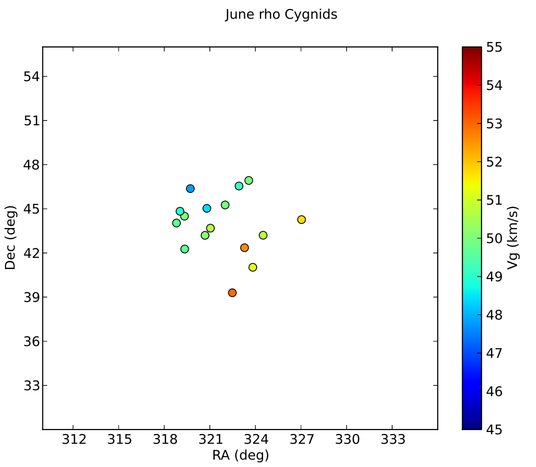

Figure 2 – Radiant plot of June ρ Cygnids.

2.3 15 Lyncids – 511 FLY

This shower is active from October 10 to October 24, but the activity is low, resulting from only 18 known orbits of this shower. The radiant plot is scattered (Figure 3), but this is expected with such a low number of orbits. The spread in radiant data and orbital elements is moderate, and a very rough estimate of mean daily motion of the radiant can be obtained: ΔRA $\approx 1.3°$/day, ΔDEC $\approx -0.1°$/day.

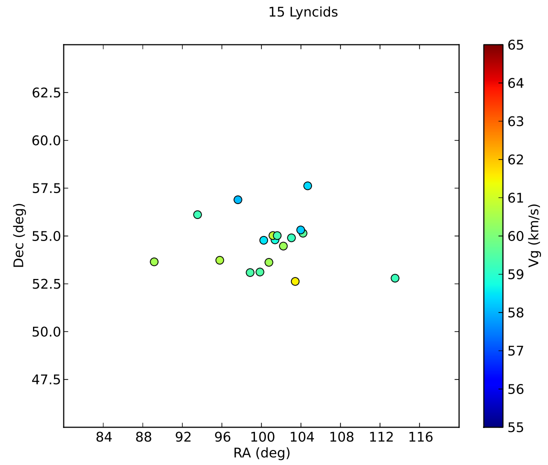

Figure 3 – Radiant plot of 15 Lyncids.

2.4 ρ Puppids – 512 RPU

The 16 orbits of this stream are spread over a time period of about 11 days, showing a nice, tidy radiant plot with large daily motion in right ascension (Figure 4). The shower is active from October 30 to November 10. The mean orbit is well defined and the mean daily motion of the radiant is roughly ΔRA $\approx 0.8°$/day, ΔDEC $\approx -0.2°$/day.

Comet C/1879 M1 (Swift) has been found to be a possible parent body of 512 RPU, with $D_{SH} = 0.18$. Comparison of orbital data is presented in Table 2. According to the JPL database, C/1879 M1 (Swift) has eccentricity equal to 1, meaning we are dealing with a comet on a parabolic orbit. But if this comet is the parent body of 512 RPU, then C/1879 M1 (Swift) is a long period periodic comet – since no uncertainty data on the comet's orbital parameters are available, this could still be true.

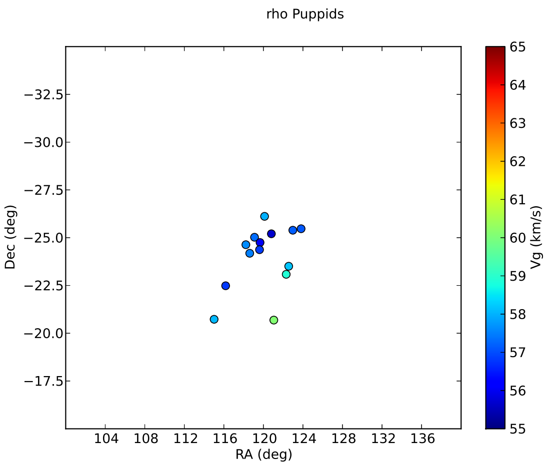

Figure 4 – Radiant plot of ρ Puppids.

Table 2 – Comparison of orbital elements of ρ Puppids (mean orbit) and the orbit of comet C/1879 M1 (Swift).

parameter	512 RPU	C/1879 M1 (Swift)
q	0.985	0.897
e	0.913	1.000
ω	9	3.8
Ω	43	47.5
i	106.4	107.0

2.5 ε Virginids – 513 EPV

Another long lasting shower with a lot of known orbits (77). The meteors of this shower span the time period from November 27 to December 18. The radiant plot nicely shows the effects of daily motion (Figure 5) with

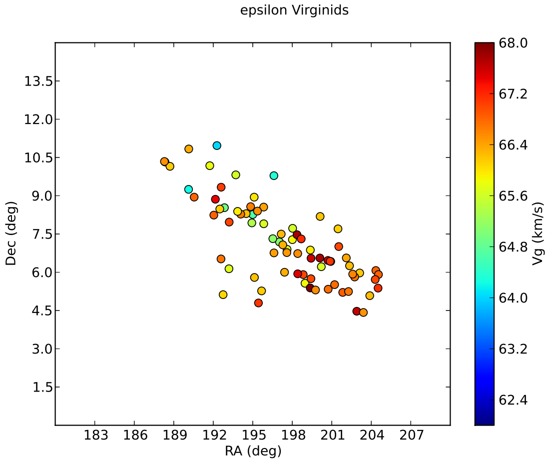

Figure 5 – Radiant plot of ε Virginids.

ΔRA $= 0.79°$/day, ΔDEC $= -0.24°$/day. The mean orbit is also well defined.

The last check of the IAU MDC and the literature revealed that this shower is already known under the name December σ Virginids (428 DSV), reported in 2012 by Greaves (Greaves, 2012). However, our data indicate a period of activity of considerably longer duration than the one given by Greaves, without overlapping with the period quoted by Greaves (the activity of 513 EPV ends 3 days before the beginning of the main concentration of 428 DSV, as quoted by Greaves). However, in the table of orbits (Greaves, 2012, Table 1), solar longitudes of the observed meteors are in the range 262°.3 – 270°.0, thus the end of the observed period of 513 EPV overlaps with the beginning of the period of 428 DSV. Based on the similarity of the mean orbits, we are dealing with one and the same shower with a long period of activity, but we will leave this to the IAU MDC to settle. The shower is also recently described by Shiba & Ueda (2013) with an even larger period of activity: December 1 to January 10 (but this article was published too late to be included in our analysis).

It is interesting to note that our analysis revealed 3 orbits with $D_{SH} < 0.15$, but with a different radiant and activity period. This could mean that the stream intersects the Earth's orbit twice, a very interesting case. We thus include this 'twin shower' in our list, with the proposed name ω Capricornids (514 OMC). The three known orbits cover the time span between May 19 to June 6.

Greaves (2012) also identifies a possible parent body, comet C/1846 J1 (Brorsen). Our parent body search confirmed this connection too, with $D_{SH} = 0.112$. The comparison of orbital data is presented in Table 3. The similarity of the orbits is striking, thus the probability of physical connection between the stream and the comet is quite high.

Table 3 – Comparison of orbital elements of ε Virginids (mean orbit) and the orbit of comet C/1846 J1 (Brorsen)

parameter	513 EPV	C/1846 J1 (Brorsen)
q	0.573	0.634
e	0.980	0.990
ω	99	99.7
Ω	258	264.0
i	151	150.7

2.6 o Leonids – 515 OLE

This shower is also active over a long time period of about a month, from January 2 to January 28, but 38 known orbits are enough for good data on the mean orbit and mean daily motion of the radiant: ΔRA $=$ $0.67°$/day, ΔDEC $= -0.27°$/day. The radiant plot (Figure 6) also clearly shows the effects of daily motion of a compact radiant.

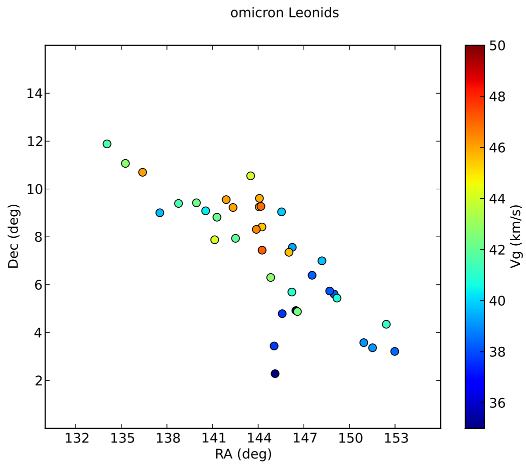

Figure 6 – Radiant plot of o Leonids.

2.7 February μ Virginids – 516 FMV

Another weak shower with moderate duration, from February 7 to February 27. The radiant plot (Figure 7) again shows clear effects of daily motion, but more data are needed to define it better. The rough values for daily motion are ΔRA $\approx 0.8°$/day, ΔDEC $\approx -0.4°$/day. Note that geocentric velocity is very well defined for this shower, which may indicate a relatively young shower.

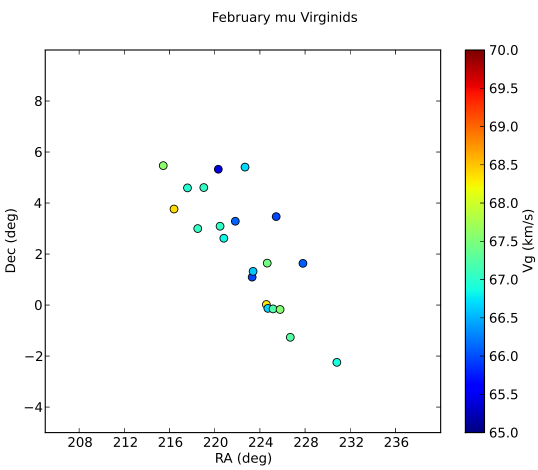

Figure 7 – Radiant plot of February μ Virginids.

Table 4 – Mean orbits of the new showers. ID is the IAU identification of the shower, name the proposed name of the shower, $\lambda_\odot$ solar longitudes between which the shower was active, RA and DEC are coordinates of the mean radiant, v_g is geocentric velocity, a is the semimajor axis of the orbit, q perihelion distance, e eccentricity, ω argument of perihelion, Ω longitude of ascending node, i inclination and N is the number of known orbits belonging to the corresponding shower. The $\pm$ values are standard deviation of the meteors selected for the corresponding shower. Note that in the case of RA and DEC there is a contribution of the daily motion to the dispersion of the radiants.

ID	name	$\lambda_\odot$	RA	DEC	v_g	a	q	e	ω (peri)	Ω (node)	i	N
509 KVI	κ Virginids	345–25	208 ± 10	-8 ± 4	37.4 ± 2.1	2.5	0.139 ± 0.039	0.938 ± 0.023	321 ± 6	6 ± 11	8 ± 4	58
510 JRC	June ρ Cygnids	81–90	321.8 ± 2.3	43.9 ± 2.0	50.2 ± 1.4	21	1.007 ± 0.005	0.931 ± 0.047	190 ± 3	84.2 ± 1.7	90 ± 3	16
511 FLY	15 Lyncids	193–211	101 ± 5	54.6 ± 1.3	59.6 ± 1.0	3.6	0.853 ± 0.023	0.755 ± 0.045	228 ± 4	202 ± 4	121.6 ± 2.3	18
512 RPU	ρ Puppids	217–228	120.0 ± 2.4	-24.0 ± 1.6	57.5 ± 1.1	13	0.985 ± 0.005	0.913 ± 0.062	9 ± 4	43 ± 3	106.4 ± 2.3	16
513 EPV	ε Virginids	245–267	197 ± 4	7.2 ± 1.6	66.4 ± 0.8	28	0.573 ± 0.034	0.980 ± 0.040	99 ± 4	258 ± 3	151 ± 2	77
514 OMC	ω Capricornids	59–73	315	-30	64.6 ± 0.8	27	0.535 ± 0.023	0.982 ± 0.032	87 ± 4	246 ± 6	142.4 ± 0.1	3
515 OLE	o Leonids	281–308	144 ± 4	7 ± 3	41.5 ± 3.8	1.8	0.079 ± 0.029	0.968 ± 0.029	151 ± 6	116 ± 6	23 ± 4	38
516 FMV	February μ Virginids	318–338	223 ± 4	2.2 ± 2.2	66.9 ± 0.7	16	0.770 ± 0.028	0.929 ± 0.039	237 ± 4	327 ± 5	146 ± 3	21

3 Conclusions

Altogether 8 new showers were discovered in the combined CMN (2007–2010) and SonotaCo (2007–2011) databases, 6 of which seem to be genuine, one is suspected (514 OMC) and one is probably already known (513 EPV may be 428 DSV). The main properties of individual showers are discussed in the appropriate sections above.

The case of 513 EPV stresses the need for the IAU MDC to be more frequently updated and to include data about the whole period of activity, as it is the main tool we have to check our findings against already known showers. Some search tools for it would also be of great help to researchers. We have written a web tool for stream searches of the MDC database and it can be accessed at:
`http://cmn.rgn.hr/in-out/search.html`

Acknowledgments

Our acknowledgments go to all members of the Croatian Meteor Network, in alphabetical order (given name first): Alan Pevec, Aleksandar Borojević, Aleksandar Merlak, Alen Žižak, Berislav Bračun, Dalibor Brdarić, Damir Matković, Damir Šegon, Dario Klarić, Dejan Kalebić, Denis Štogl, Denis Vida, Dorian Božićević, Filip Lolić, Filip Novoselnik, Gloryan Grabner, Goran Ljaljić, Ivica Ćiković, Ivica Pletikosa, Janko Mravik, Josip Belas, Korado Korlević, Krunoslav Vardijan, Luka Osokruš, Maja Crnić, Mark Sylvester, Mirjana Malarić, Reiner Stoos, Saša Švagelj, Sonja Janeković, Tomislav Sorić, VSA group 2007, Zvonko Prihoda, Željko Andreić, Željko Arnautović, Željko Krulić. Also, to Peter Gural for constructive discussions on meteor shower problems.

This work was partially supported by the Ministry of Science, Education and Sports of the Republic of Croatia, Višnjan Science and Education Center and by private funds of CMN members.

References

Andreić Ž. and Šegon D. (2010). “The first year of Croatian Meteor Network”. In Kaniansky S. and Zimnikoval P., editors, *Proceedings of the International Meteor Conference, Šachtička, Slovakia, 18-21 September 2008.* International Meteor Organization, pages 16–23.

Andreić Ž., Šegon D., and Korlević K. (2010). “The second year of Croatian Meteor Network”. In Andreić Ž. and Kac J., editors, *Proceedings of the International Meteor Conference, Poreč, Croatia, 24-27 September 2009.* International Meteor Organization, pages 26–30.

Greaves J. (2012). “Four meteor showers from the SonotaCo Network Japan”. *WGN, Journal of the IMO*, **40:1**, 16–23.

IMO (1993–2012). “IMO Video Meteor Database”. `http://www.imonet.org/database.html` .

Jenniskens P., Jopek T. J., Rendtel J., Porubčan V., Spurný P., Baggaley J., Abe S., and Hawkes R. (2009). “On how to report new meteor showers”. *WGN, Journal of the IMO*, **37:1**, 19–20.

Jopek T. J. and Froeschlé C. (1997). “A stream search among 502 TV meteor orbits. An objective approach”. *Astron. Astrophys.*, **320**, 631–641.

Korlević K., Šegon D., Andreić Ž., Novoselnik F., Vida D., and Skokić I. (2013). “Croatian Meteor Network catalogues of orbits for 2008 and 2009”. *WGN, Journal of the IMO*, **41:2**, 48–51.

Shiba Y. and Ueda M. (2013). “December σ-Virginids”. *WGN, Journal of the IMO*, **41:1**, 7–10.

SonotaCo (2005–2012). “SonotaCo Network simultaneously observed meteor data sets”. `http://sonotaco.jp/doc/SNM/index.html` .

Southworth R. B. and Hawkins G. S. (1963). “Statistics of meteor streams”. *Smithsonian Contr. Astrophys.*, **7**, 261–285.

Šegon D., Andreić Ž., Korlević K., Novoselnik F., and Vida D. (2012a). “Croatian Meteor Network catalogue of orbits for 2007”. *WGN, Journal of the IMO*, **40:3**, 94–97.

Šegon D., Andreić Ž., Korlević K., Gural P., Novoselnik F., Vida D., and Skokić I. (2012b). “New shower in Cassiopeia”. *WGN, Journal of the IMO*, **40:6**, 195–200.

Handling Editor: David Asher
This paper has been typeset from a LaTeX file prepared by the authors.

“Thatcher’s Ghost”: Confirmation of the ν Cygnids (NCY, IAU #409)

Peter Jenniskens and Bob Haberman [1]

A ghostly image of meteor radiants appeared in the CAMS data north-east of the Lyrids on April 22, 2012. The diffuse shower is identified as the ν Cygnids (NCY). It is weakly active from April 17 to 26, and likely related to the April ρ Cygnids (ARC), active in the area after April 27. The ν Cygnids may have been in outburst in 2012, because this shower was not as evident in the 2007–2011 SonotaCo data.

Received 2013 January 8

1 Introduction

During the peak of the Lyrid shower in late April 2012, weather in northern California was clear from April 15 through 23. CAMS (Jenniskens et al., 2011) measured 1362 orbits. In the daily maps of April 22, a ghostly image of meteor radiants appeared just north-east of the Lyrid radiant (Figure 1). The shower was strong only in two nights, at solar longitudes of $30\overset{\circ}{.}0 - 32\overset{\circ}{.}0$, but weak activity was present in the area from April 17 to 26 (solar longitude $27\overset{\circ}{.}4 - 36\overset{\circ}{.}6$). It was weak too in the 2011 April 21 CAMS data.

2 The available data

Despite being relatively diffuse compared to the Lyrid radiant, the shower may have been in outburst, because it was not detected in the 2007–2011 SonotaCo data of solar longitudes $30^\circ - 32^\circ$ (Figure 1). Reason for that may be simply because of the lower number of total meteors captured (154), less than the 447 measured by CAMS in this period. On the other hand, there is only a weak detection of this shower when averaged over period $27\overset{\circ}{.}4 - 36\overset{\circ}{.}6$ (997 meteors).

This does not appear to be a manifestation of the April ρ Cygnids (Figure 2). That shower was detected by CMOR in the period April 25 to May 4 (Brown et al., 2010) and confirmed by 2011 CAMS data in the period April 27 to May 7 (Phillips et al., 2011), or solar longitude $35^\circ - 47^\circ$. The ARC radiant drift was measured as $0.67^\circ/^\circ$ in R.A. and $+0.1^\circ/^\circ$ in Decl. That would put the radiant at $\alpha = 317\overset{\circ}{.}3$, $\delta = +46\overset{\circ}{.}8$ at solar longitude $31\overset{\circ}{.}6$. The observed radiant is 7° lower in R.A. and 6° lower in Decl. (Table 1).

3 Comparing with past observations

The shower is not unknown. When compared to the IAU Meteor Shower Working List, we find good agreement with the ν Cygnids (NCY, IAU#409), found from IMO single-station video data by Molau and Rendtel (Molau & Rendtel, 2009). Based on 508 meteors, that shower peaked at solar longitude 30°, with an observed radiant at $\alpha = 305\overset{\circ}{.}2$, $\delta = +39\overset{\circ}{.}4$, $v_\infty = 42$ km/s. Due to confusion with the ARC shower, a steep radiant drift of $+1.8^\circ/^\circ$ in R.A. and $+0.7^\circ/^\circ$ in Decl. was found and a long activity period $(28^\circ - 44^\circ)$.

Both showers are likely from the same source. Just like the ARC, the ν Cygnids have a short-period Jupiter family comet semi-major axis of $a \sim 3.7$ AU (range $2 - 14$ AU). ARC has $a \sim 5.6$ AU (Phillips et al., 2011). Longitude of perihelion are $\varpi = 168\overset{\circ}{.}9$ and $170\overset{\circ}{.}3$, respectively. The difference in radiant position could be simply due to perturbations of the comet orbit in close encounters with Jupiter. If the ν Cygnids were in outburst in 2012, they may represent the more recent cometary activity.

4 Acknowledgement

We thank Jim Albers (Sunnyvale), Bryant Grigsby (Lick Observatory), and Rick Morales (Fremont Peak Observatory) for supporting the operation of the CAMS stations. This work is funded by the NASA/NEOO program.

References

Brown P., Wong D. K., Weryk R. J., and Weigert P. (2010). “A meteoroid steam survey using the Canadian Meteor Orbit Radar. II: Identification of minor showers using a 3D wavelet transform”. *Icarus*, **207**, 66–81.

Jenniskens P., Gural P. S., Dynneson L., Grigsby B., Newman K. E., Borden M., Koop M., and Holman D. (2011). “CAMS: Cameras for Allsky Meteor Surveillance to validate minor meteor showers”. *Icarus*, **216**, 40–61.

Molau S. and Rendtel J. (2009). “A comprehensive list of meteor showers obtained from 10 years of observations with the IMO Video Meteor Network”. *WGN, Journal of the IMO*, **37:4**, 98–121.

Phillips M., Jenniskens P., and Grigsby B. (2011). “Confirmation of the April Rho Cygnids (ARC, IAU#348)”. *WGN, Journal of the IMO*, **39:5**, 131–136.

Handling Editor: Paul Roggemans

[1] SETI Institute, 189 Bernardo Ave., Suite #100 Mountain View, CA 94043, United States
Email: `petrus.m.jenniskens@nasa.gov`

IMO bibcode WGN-413-jenniskens-nu-cygnids
NASA-ADS bibcode 2013JIMO...41...75J

Table 1 – The geocentric radiant, speed, and orbit in interval of solar longitude 30°.0 – 32°.0, with errors showing the standard deviation dispersion. Second row gives the median error in individual measurements.

Shower	α_g [°]	δ_g [°]	v_g [km/s]	q [AU]	$1/a$ [AU^{-1}]	i [°]	ω [°]	Ω [°]	N
NCY (CAMS)	309.9 ± 5.3	41.3 ± 2.2	43.3 ± 3.2	0.893 ± 0.046	0.27 ± 0.20	74.6 ± 4.4	137.3 ± 9.6	31.6 ± 0.5	37
σ	± 0.7	± 0.8	± 0.9	± 0.0053	± 0.042	± 0.69	± 1.3	± 0.0004	
NCY (IMO)[1]	305.8	39.4	40.4	—	—	—	—	30.0	508
Lyrids (CAMS)	271.2 ± 2.0	33.8 ± 1.2	46.7 ± 1.3	0.920 ± 0.017	0.037 ± 0.037	79.0 ± 1.8	214.1 ± 4.0	31.6 ± 0.5	110
Lyrids (Son.)	271.6 ± 1.8	33.5 ± 1.0	46.4 ± 1.8	0.918 ± 0.015	0.060 ± 0.124	79.1 ± 2.1	214.9 ± 4.1	31.8 ± 0.5	57
ARC (CAMS)[2]	324.5	45.9	41.8	0.844 ± 0.034	0.18 ± 0.10	69.7 ± 2.8	130.4 ± 6.2	39.9 ± 2.9	29

[1](Molau & Rendtel, 2009); [2](Phillips et al., 2011)

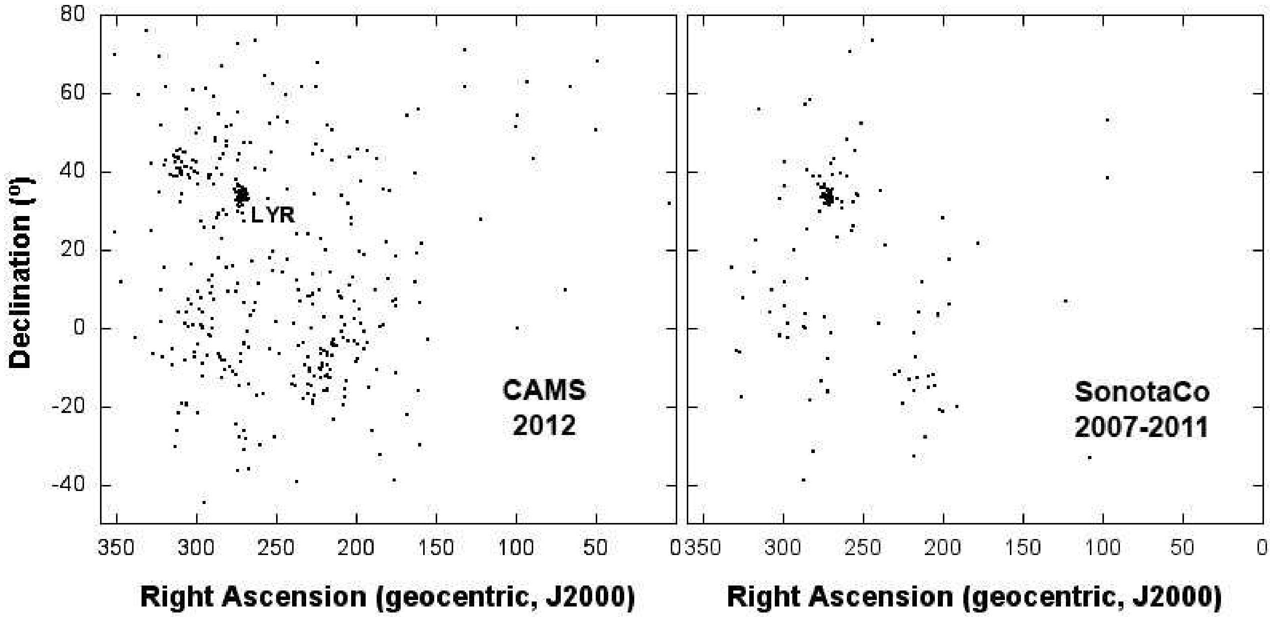

Figure 1 – The ν Cygnids is the group north-east of the Lyrid radiant in the CAMS April 22 data.

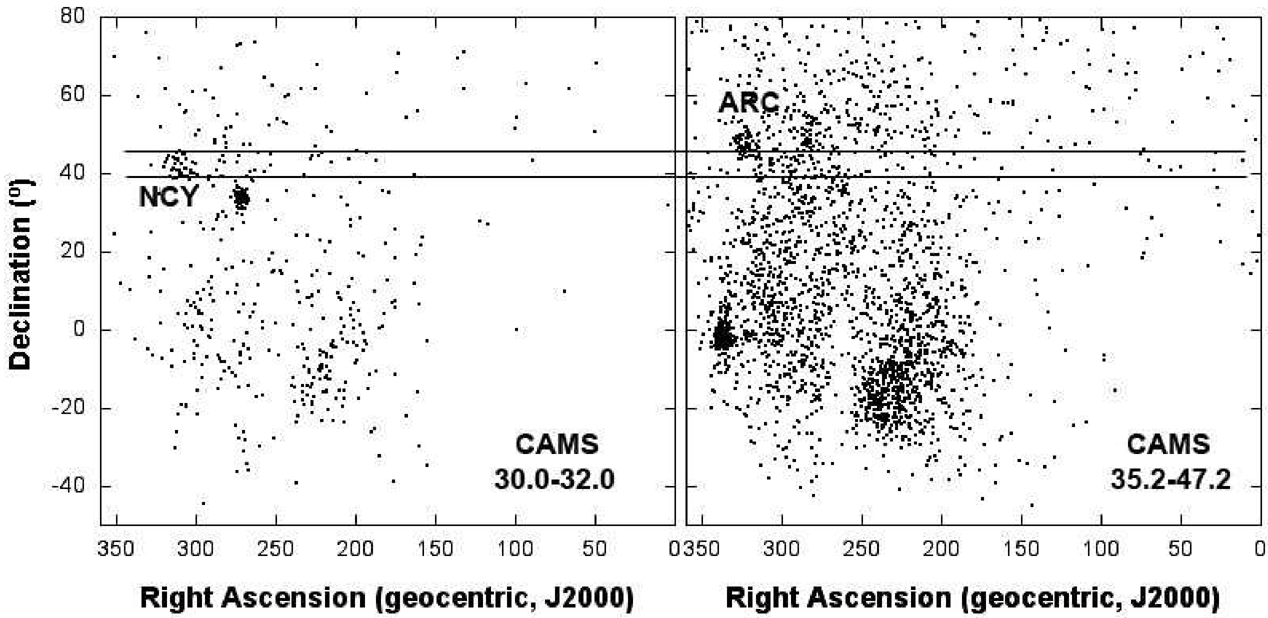

Figure 2 – CAMS data in two time intervals, with NCY and ARC showers marked.

Ongoing meteor work

Comet 17P/Holmes: originally widely spreading dust particles from the 2007 explosion converge into an observable dust trail near the common nodes of the meteoroids' orbits

Esko Lyytinen[1], *Markku Nissinen*[2], *Harry J. Lehto*[3]

Meteoroids were ejected in the 2007 explosion of comet 17P/Holmes. They experienced a spread into elliptic orbits around the Sun. The cloud widened and apparently vanished altogether. We have now re-discovered this swarm of meteoroids. At exactly the opposite side of the Sun, the meteoroids converge again around the mutual node of the orbits (where the orbital planes cross each other). Later the particles re-converge at the original explosion site, all passing through the "point of explosion". Because of differences in the orbits this passage through the convergence point lasts for quite a while, maybe around two years. In spite of the long duration, the increase in surface brightness around these regions is expected to be enough to be observable in visible light. It could be observed as thermal IR in the mid infrared (15–25μm) corresponding to temperatures 200K–120K expected at distances 2AU–5AU, between the perihelion and the aphelion of the comet. We present here our observations on two nights of February 2013. We observed the meteoroids at the far away node, which is opposite of the explosion site relative to the Sun. The comet itself passed the observed region a little more than two-and-a-half months earlier in late December 2012. This why the February 2013 observations had a better chance of success than observing the same spot on previous years as the meteoroids would had not reached this spot earlier. Another probably more prominent convergence is expected to happen at the 2007 explosion site. As seen from Earth it will appear to be at a different place in the sky than the 2007 outburst. We predict this to be observable starting in the autumn of 2013, probably around November and continuing for about two years. Based on the expected dispersion in the orbits and a purely gravitational solution we expect the effect to last almost two years, but due to solar radiation pressure, it will probably continue longer (Burns & Lamy, 1979). Observing both or either of these future convergences will give further information about the explosion itself and the effects of solar radiation pressure on particles of different sizes. Such information may be useful in the development of meteor outburst prediction models.

Received 2013 May 14

1 Introduction

Comet 17P/Holmes underwent a massive outburst on 2007 October 23. This was the largest recorded cometary outburst releasing large quantities of gas and dust (Sekanina, 2009; Montalto et al., 2008; Ishiguro et al., 2010). The dust particles from this explosion entered into several different orbits that are similar but not identical to the orbit of the comet. The orbital elements of each individual meteoroid orbit may vary in all aspects, but for our research the differences in orbital planes are of special importance. The shape of the orbit is further affected by solar radiation pressure. This pressure is proportional to the inverse of the distance squared from the Sun and it causes a force component pointed away from the Sun. It lengthens the orbital periods, in principle to some degree for all particles and drives the smallest particles into hyperbolic orbits.

Particles smaller than a few microns will go to hyperbolic, although particles much smaller than the solar radiation effective wavelengths may not do this.

The ratio of the radiation force to the gravitational pull is denoted as β. For a given particle (assuming similar properties like density and reflecting properties), the value of β is inversely proportional to the diameter, except when the size is clearly smaller than the radiation wavelength. We consider a mm size particle to have a beta value of $\beta = 0.001$ (Burns & Lamy, 1979).

An important issue here is that β does not affect the orbital planes and also do not divert particles away from passing through the explosion site (if not pushed to very long or hyperbolic orbits). The orbit geometry remains a conic section orbit.

After one revolution of 6.9 years (orbital period of the comet), the particles on elliptic orbits should converge in space at the explosion site. As calculated from a spherical symmetric explosion with maximum ejection velocity of 0.5 km/s, individual particles will have orbital periods from 6.06 to 7.94 years. But solar radiation pressure will lengthen the orbital periods of small size particles to infinity, in theory. We call the solutions that assume a zero radiation pressure, as "purely gravitational solution". For example the above values 6.06 and 7.94 years are from such a solutions. Radiation pressure properties in which the simple regular model

[1]Kehäkukantie 3 B, 00720 Helsinki, Finland. Email: esko.lyytinen@jippii.fi
[2]Kirvesniementie 24 B, 78880 Kuvansi, Finland. Email: markku.nissinen@pp.inet.fi
[3]Tuorla Observatory, University of Turku, 21500 Piikkiö, Finland. Email: hlehto@utu.fi

IMO bibcode WGN-413-lyytinen-holmes
NASA-ADS bibcode 2013JIMO...41...77L

are not adequate, were discussed in our earlier papers (Lyytinen & Van Flandern, 2000; Lyytinen et al., 2001).

The most immediate convergence will happen in the near-side common node of the meteoroids, which is the explosion site. Differences in the orbital periods of the orbits, will mainly cause a spread in the timing. Differences in other orbital elements, (e.g. in orbital planes) will cause an hour-glass shape.

Minor effects (such as the fact that the explosion was not quite momentary and the influence of differential planetary perturbations, and some expected departures of the radiation pressure from the simple model) affect the exact location of individual particles near common nodes causing some spread to the width of the hour-glass center width. Planetary perturbations will also slightly shift the location.

We expect that the increased number of small meteoroids in the limited volume of space will cause a small and local increase in the sky background. This node crossing is spatially quite narrow. The above mentioned limits of the orbital period in principle determine the duration of the phenomenon. Because of the radiation pressure, the upper limit is not well defined but we expect the observing window to last maybe a lot more than two years, and keep recurring for several successive orbital revolutions. Although it is not at all certain if this is bright enough to be observable during these successive revolutions. We cannot now predict how long the hour-glass of one revolution will be observable and to what degree the successive revolution convergences can be observed. And these are dependent on the observing equipment.

As a first approximation (i.e. without perturbations), every elliptic orbit stays fixed also in the next revolutions. When affected by the solar radiation pressure (to some approximation level) the orbits will be kept as conic sections and consequently, if not pushed into parabolic or hyperbolic orbits, will also be in elliptic orbits. The assumption of a "point-like" explosion in space and in time (which it of course is not actually) implies that every particle remains in an elliptic orbit and it will later pass trough the explosion site according to this level of approximation. This is expected to be sufficient level of accuracy for explaining a general view of the phenomenon, although the orbit is further in reality altered by planetary perturbations for example, and by the fact that the explosion was not quite point-like.

There is a second common node, the far-side node, which is located on the orbit at exactly the opposite side of the Sun. The transit of meteoroids close to this point differ in one important respect: the individual meteoroids have a significantly wider dispersion in the orbital radii. The implication is that this common node can be detected optically only when the Earth is close to the comet's orbital plane, which is when the dispersive effect of the radial spread is minimized. Such a node crossing occurred on 2013 February 15. The observing window of the far side common node is expected to be a month at the most.

We distinguish two types of nodes. First, the line of common nodes of orbits of the explosion material: we refer to two locations along this line as the near-side node and far-side node. Second, the points at which the Earth crosses the comet's orbital plane: the Earth reaches these points in February and August.

Because of the changing geometries between the orbit of the comet and Earth, the positions of both nodes vary in the sky and are not located on the ecliptic nor at the same position as the 2007 apparent orbit.

The first time we are aware envisioning the possibility of this kind of a phenomenon, that we know of was in the Finnish language magazine *Tähdet ja Avaruus* in an article of the comet explosion by Mikko Suominen and interview of Esko Lyytinen (Suominen, 2007). An approximate English translation of this is: Esko Lyytinen expects that at the next revolution, a phenomenon "shaped like an hour-glass" may appear at the explosion site. It could be visible for a long time. Probably it cannot be observed with amateur instruments, but space-telescopes may have success. "As the comet appears very interesting now, it could be research wise even more interesting after around one revolution has passed".

This last sentence mainly reflects the interests of Esko Lyytinen with dust trail models for meteor outbursts predictions. And as to the observability of these phenomena we later had different thoughts of this.

2 Computer visualizations of the convergence in the common nodes

We calculated the orbits of some individual meteoroids, needed for the predictions etc, although no actual multiparticle modeling was made. No planetary perturbations were applied to the tracks. Some additional minor approximations were applied.

We modelled the explosion as spherically symmetric. We adopted the 2007 MPC or MPEC orbital elements for the comet, except that we changed the inclination to the cometary value of the epoch in 2013 (IAU MPC, 2013). The selection of the epoch has an effect of a few arc minutes on the position of the track. The comet itself passed the observed region a little more than two-and-a-half months earlier in late December 2012.

We modeled the individual meteoroid orbits as having orbital planes that differ from each other by up to 3 degrees. This is the most important factor in forming of the apparent hourglass shape.

The crossing of the planes causes a definite contraction and increase of apparent brightness at the mutual nodes. This brightening is quite noticeable, even though the time span, when the meteoroids pass by these regions is relatively long. We also estimated the surface brightness of the trail.

Figure 1 shows how the orbits seem to cross in the sky, as seen from inside the orbit close to the Sun, and close to the plane itself. The orbits form a narrow "hourglass" pattern in the sky. The opening angle shown here has been exaggerated a bit. In reality, it is expected to be around three degrees. The surface

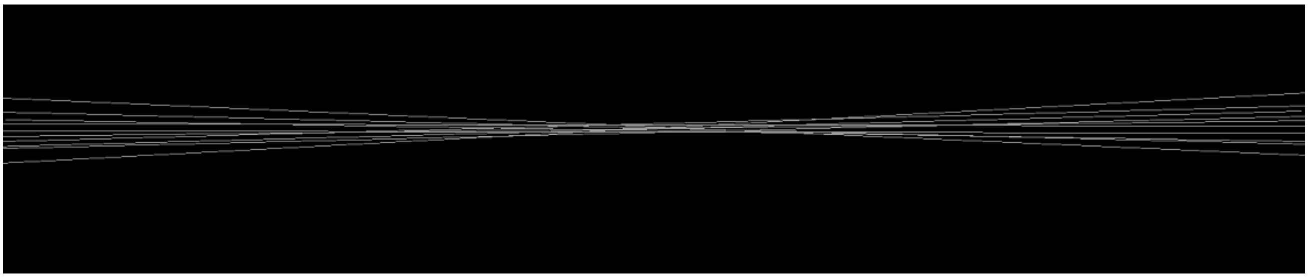

Figure 1 – Schematic diagram of how the orbits cross in the sky.

brightness increase near the crossing is the center of the common node. Of course, we cannot see the actual orbital planes but a similar figure is formed by a vast number of individual meteoroids.

As to the near side node of the explosion site, we expect the radial dispersion to be roughly equal to the normal dispersion, possibly slightly more. Since also the radial dispersion is fairly small, the observing of the convergence is not restricted to when the Earth is near the orbital plane. However, we expect the brightness distribution to have this same hourglass shape. The center is expected to be narrower and with a higher surface brightness than in the far side common node.

3 Our observations in February 2013

We carried out observations to detect the far side common node. The predicted optimum date was on 2013 February 15 but due to circumstances our observations were carried out on 2013 February 17 and 19.

We used the 32 cm T9 [1] and 51 cm T30 [2] Australia remote-controlled iTelescopes in the Siding Spring Observatory and pointed at the expected position of the trail and the hourglass figure at $16^{h}07^{m}07^{s}$, $-40°17'$ (J2000.0). The T30 is a Planewave $20''$ (0.51 m) CDK Corrected Dall-Kirkham Astrograph on a Planewave Ascension 200HR mount equipped with a FLI-PL6303E CCD. The images were unbinned and taken in white light with a Luminance filter. A $0.66\times$ focal reducer was used providing an effective focal length is 2280 mm. The total field of view was 27.8×41.6 arc minutes. We could barely see it in the images taken with the T9 telescope. The T30 turned out to be superior because of its larger size and automatic guiding, which helped tremendously in applying the image subtraction method in a very dense Milky Way star field. The observing conditions were very good on both nights and the Moon was not present. Our first set of seven 300-second exposures were taken on 2013 February 17, $16^{h}31^{m}$ UT. The second set of frames consisting of six 300-second exposures was obtained on 2013 February 19, $17^{h}21^{m}$ UT. Each night standard reductions were applied and the reduced image were averaged into one master image per night, so we had two masters with a time separation of $48^{h}50^{m}$.

Next we subtracted the February 17 master image from the February 19 master image. It was immediately obvious that the stars had been mostly removed and that the trail showed in the difference image as a positive band at the February 19.7 location and as a negative one at the February 17.7 location.

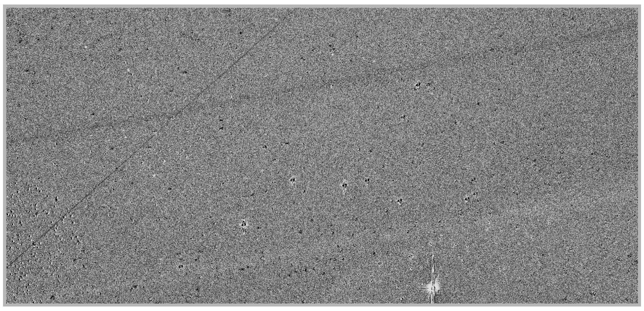

Figure 2 – The subtracted image of 2013 February 17.

The difference image is shown in Figure 2. It has been cropped to some degree so the center of the image is not exactly the original one. The center of the original image is horizontally in the center but close to the February 17.7 trail, about $40''$ to the south of the trail. North is up, but the position angle of the vertical axis (around the image center) is about 2.0 degrees off.

The horizontal width of Figure 2 is about 42 arc minutes. The meteoroid trails are seen as two broad bands in the position angle of 100 degrees. Also visible in the image are a couple of narrow satellite trails and an unknown artifact in the lower right corner. The difference image was made with Isis2.2 program (Alard, 2000). The subtraction technique proved a much more effective method than looking at master images or using other subtraction programs for detecting the trails. The critical factor was the good field star removal capability of the Isis2.2 program.

We tried to observe the trail again on the night between March 7 and 8 with a reference image taken later. We did not detect the trail. It is likely that this is due to too much time passing after the most favorable conditions of February 15 when the Earth crossed the orbital plane of the comet. Furthermore, the galactic background was even more challenging than earlier.

Our observing time was restricted on other nights by the high overall demand of the telescopes, the Moon, sky cloudiness and humidity in the morning hours. With more observing time, it would have been useful to image additional fields along the trail.

We have planned new observations for the next possibility of observing the far side node, around 2013 August 19.

[1] `http://www.itelescope.net/telescope-t9`
[2] `http://www.itelescope.net/telescope-t30`

4 Analysis of the February 2013 images

The location of the phenomenon in the sky was calculated in advance. The position of the trail was within one arc minute of the calculated location. The mutual separation of the two trails is consistent with what the calculated change of the trail track is over $48^{h}50^{m}$ to within about 10 arc seconds, which is roughly the accuracy of this comparison measurements and expected calculated ephemeris accuracy. The position angle of the tracks in the sky is within a few tenths of a degree of the calculated one, which is practically as accurate as one could measure. Considering that the position of the trail, the change in the position with time and the position angle all match calculated values, we are confident that we really have detected and imaged the trail, i.e. the cloud of meteoroids produced by 17P/Holmes at their common node.

To search for the hourglass pattern we rotated the difference image by 10.4 degrees to make the trails appear horizontal. We further smoothed and compressed the image along the trail and finally separated the two tracks into Figures 3 and 4. The hourglass shape is readily visible. The center of the hour glass in the February 17.7 image is at a distance of about 1/3 of the Figure 3 from the left-hand side. On the February 19.7 image (Figure 4) it is even closer to the left-hand edge of the image which is consistent with our calculations.

The profile across the February 17.7 trail shown in Figure 5 is the median along a 1400 pixel stretch of the trail. The stretch was centered on about the hourglass center and calculated from the original subtracted image. Optimally we would have preferred to measure the profile at the hourglass center, but to improve the signal-to-noise ratio we carried out the averaging along the trail. The horizontal direction one unit equals 0.81 arc seconds. The vertical unit is equal to that of the original subtracted image. The sky background corresponded to 785 units. We further note that the during the total covered exposure time of about 40 minutes, the trail track itself shifted about 20 arc seconds, affecting also to this profile width and shape.

The noise (standard deviation of individual pixel values in the background) in the master images is about 10 units, while the signal is only about 3 or 4 units. It appears from these numbers that the brightness (increase over the background) near the center is measured at 0.5% of the sky background. We expected this to be a challenging observation but this is even dimmer than what we thought it would be. Maybe it was fortunate that we did not accurately know its actual brightness (dimness) as we might not have even tried these observations.

5 Estimating the observed trail brightness from the observed explosion cloud brightness

The comet's apparent maximum brightness after the explosion was about magnitude 2. We start from the assumption of magnitude 2.0 and derive what the expected surface brightness in February 2013 should be if only geometry is considered, i.e. no loss of brightness from vanishing particle numbers, or change in size or surface color of the particles. Transforming the magnitude 2 brightness of the explosion to what it would be at the far node, taking into account the distance from both Earth and the Sun, and assuming the inverse square dependency on both distances, we get an expected total magnitude of 4.8. However, this has become dispersed along the trail rather than concentrated in a cloud. Starting from a supposed maximum ejection velocity of 0.5 km/s we derive from our orbit simulations that the phenomenon will last for roughly 600 days. We did not know prior to our observations what to expect of the width of the trail in the center of the hour glass. We measure this to be about 25″. During one day, a particle would move on these orbits about $0\overset{\circ}{.}148$ (532″), in true anomaly and about a similar length as seen from the Earth, if it were stationary.

Let us assume the phenomenon to have a constant brightness, provided that we could observe it from the same fixed location in the Solar system. Now we can calculate the factor of reduction in surface brightness. We get the expected surface area by multiplying $600 \times 532 \times 25$ which equals about 8.0 million square arc seconds. We can now divide the assumed brightness by 8.0 million square arc seconds. This factor is equals to 17.3 magnitudes, giving a value of $4.8 + 17.3 = 22.1$

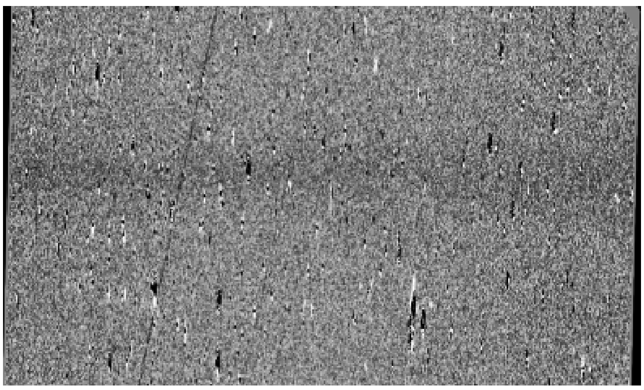

Figure 3 – The trail observed on 2013 February 17, rotated and reduced in length.

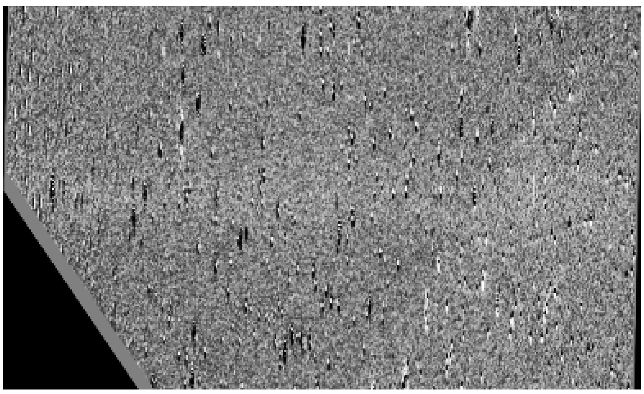

Figure 4 – The trail observed on 2013 February 19, rotated and reduced in length.

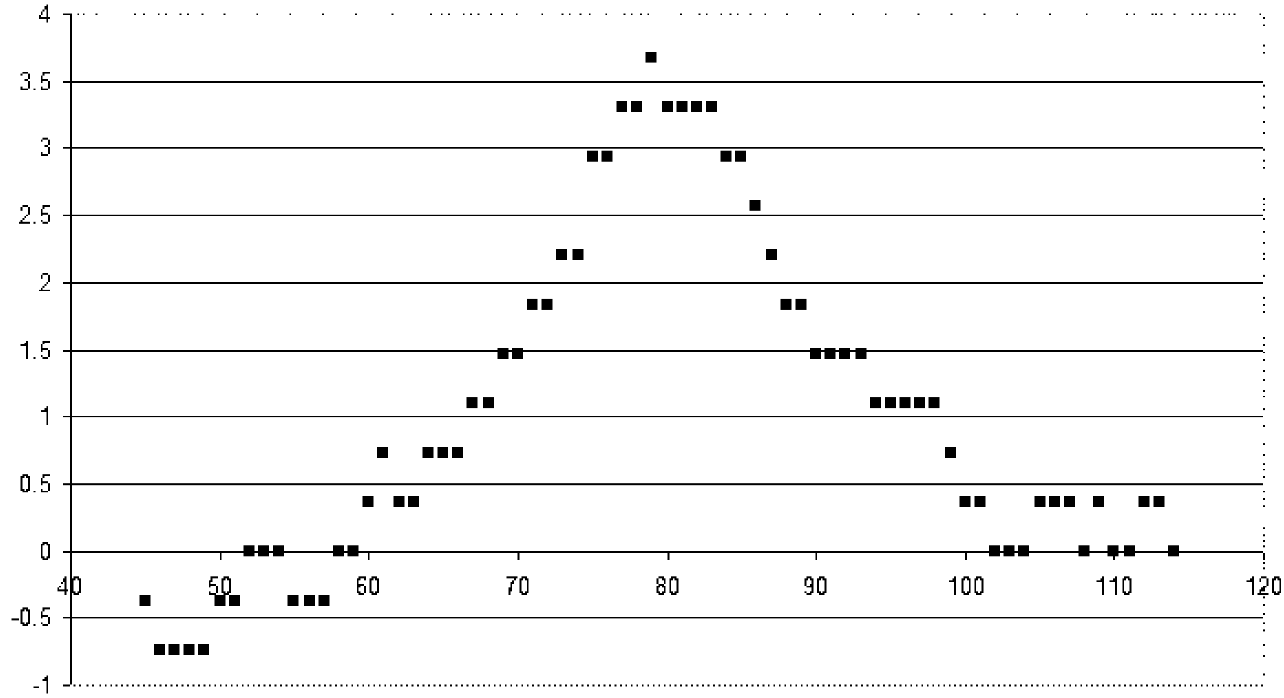

Figure 5 – Profile of the trail on February 17. Horizontal axis is in units of 0.″81 (plate scale of the image) and the zero point is arbitrary. The vertical axis has the same units as the original image (ADU), with the background value of 785 removed. Each point is a median along a 1400 pixel long stretch of the trail. The profile was further smoothed by a 5 pixel running average along the profile. The width of the trail is consistent with to the expected width of 25″ (30 pixels).

magnitudes per square arc second. This is to be added to the sky background. The brightness in our observations is obtained by assuming the sky background of 21.0 mag/square arc second, in this Milky Way region. This value is our assumption. The measured brightness of 0.5% relative to the background is equal to 26.8 mag/square arc second. It appears that there is a 4.7 mag, or about 70 fold, reduction in the brightness as compared to the calculation with no loss assumed. The total brightness of the comet is partially due to water vapor and other volatile gases that escape quickly. Small ice particles evaporate in the coma at a short distance from the comet nucleus (Stevenson & Jewitt, 2012). Dust or meteoroid particles of ice mixed with organics and minerals tend to become darker, lowering the albedo (Stevenson & Jewitt, 2012). Furthermore, larger particles are likely to fragment. Alternatively, it is conceivable that the brightness of the coma is determined by the larger particles and meteoroids (1 cm to meters) but they are much fewer in number than the smaller particles (Fulle, 2004). This would reduce the estimated number of particles entering the calculated orbits right from the beginning.

The assumed duration of 600 days of the spread of the trail is close to the purely gravitational solution. If an especially big proportion of the ejected particle mass is in the form of very small particles, say around 0.01 mm and smaller, then the duration may be considerably longer than that 600 days. Micron-size particles will get into hyperbolic orbits after the ejection and are essentially lost. We expect the larger meteoroids to head the trail and the smaller particles to make an ever thinner, dimmer and long lasting trail. Thermal infrared and radar observations could yield insight into the length and size distribution of the particles in the trail.

6 Future observable phenomena

The next time the Earth is in the orbital plane of 17P/Holmes is on 2013 August 19 or 20. The trail is located at about 13^h55^m, $-31°$. It is observable from southern locations in the evening sky right after twilight. We expect the hourglass to be observable for about a week on both sides of this, possibly longer. The apparent location changes daily. The detailed predictions are shown in Table 1. Because we are anticipating to repeat our observations at Siding Spring, we have given the coordinates for 12 UT of the given dates. Rough interpolations of the coordinates are good

Table 1 – Predictions of the "hourglass center" coordinates in August 2013.

Day	Right Ascension	Declination
05.50	$13^h49.11^m$	$-31.°77$
10.50	$13^h50.64^m$	$-31.°50$
13.50	$13^h51.71^m$	$-31.°35$
15.50	$13^h52.48^m$	$-31.°26$
17.50	$13^h53.32^m$	$-31.°19$
19.50	$13^h54.20^m$	$-31.°11$
21.50	$13^h55.12^m$	$-31.°05$
23.50	$13^h56.10^m$	$-31.°00$
25.50	$13^h57.10^m$	$-30.°95$
30.50	$13^h59.82^m$	$-30.°86$

enough for imaging. We used true anomaly of 241.25 degrees to generate Table 1. This value corresponds to the comet 2007 orbit but the actually used values for meteoroid orbits differ from this, because of differences in the argument of perihelion. We expect that the uncertainty of the center along the trail may be as much as a few tenths of a degree. The stellar background will be much more favorable in August than what it was in February. Unfortunately, the full moon will be a problem. After this the next time Earth will cross the comet's orbital plane will be in February 2014. The hourglass phenomenon in this mutual node would have ended before this, based on a purely gravitational solution. But because of solar radiation pressure, we expect it to still continue on that date. We are going to inform separately about the refined predictions for February 2014.

The convergence to the actual explosion site is also starting soon. Based on the maximum ejection velocity value of 0.5 km/s opposite to the comet's velocity vector, we predict that this will take place on about 2013 November 12. If the velocity were 0.45 km/s it would begin almost a month later. Radiation pressure may slightly delay the start date. It would be optimal if the start of the convergence could be observed. It will be observable in the northern hemisphere. The start is expected to be quite sudden, but will probably not be at full brightness. A pure gravitational solution would give the duration of the convergence through this site close to 700 days, but because of radiation pressure, we expect this to last a lot longer, possibly with an undetermined end and perhaps lasting for a number of years.

The predicted coordinates for the explosion site convergence are given in Table 2. The same coordinates can be used for the year 2015, using the same solar longitude. Then these same coordinates will be valid at about 06^{h} UT on the same dates.

After two or three revolutions one could, in principle, observe the two tracks simultaneously and somewhat separated by planetary perturbations. But it is uncertain if the brightness will be sufficient enough for any actual observations.

In all these future scenarios, we have assumed that practically all the loss of the meteoroids has already happened and there will not be much further loss. If further break up and consequent vanishing of particles takes place, then the brightness of the phenomena will decrease. This would provide important information on the break-up of small particles and meteoroids in interplanetary space.

7 Conclusion

We documented the swarm of meteoroids in the orbit of comet 17P/Holmes. A low surface brightness trail was detected at the calculated position at the correct position angle and the expected motion and shape.

We recommend additional observations of these meteoroids from Southern hemisphere locations in August 2013 and from Northern hemisphere locations from October 2013 onwards.

Table 2 – Predictions for the explosion location. Because of missing planetary perturbations, these can be in error by a few hundredths of a degree.

Date (0^{h}UT) yyyy mm dd	Right Ascension	Declination
2013 10 05	$4^{\mathrm{h}}38.12^{\mathrm{m}}$	$+47\overset{\circ}{.}78$
2013 10 10	$4^{\mathrm{h}}28.86^{\mathrm{m}}$	$+48\overset{\circ}{.}57$
2013 10 15	$4^{\mathrm{h}}17.43^{\mathrm{m}}$	$+49\overset{\circ}{.}25$
2013 10 20	$4^{\mathrm{h}}03.83^{\mathrm{m}}$	$+49\overset{\circ}{.}78$
2013 10 25	$3^{\mathrm{h}}48.17^{\mathrm{m}}$	$+50\overset{\circ}{.}09$
2013 10 30	$3^{\mathrm{h}}30.80^{\mathrm{m}}$	$+50\overset{\circ}{.}12$
2013 11 04	$3^{\mathrm{h}}12.26^{\mathrm{m}}$	$+49\overset{\circ}{.}82$
2013 11 09	$2^{\mathrm{h}}53.30^{\mathrm{m}}$	$+49\overset{\circ}{.}17$
2013 11 14	$2^{\mathrm{h}}34.71^{\mathrm{m}}$	$+48\overset{\circ}{.}16$
2013 11 19	$2^{\mathrm{h}}17.23^{\mathrm{m}}$	$+46\overset{\circ}{.}84$
2013 11 24	$2^{\mathrm{h}}01.41^{\mathrm{m}}$	$+45\overset{\circ}{.}27$
2013 11 29	$1^{\mathrm{h}}47.59^{\mathrm{m}}$	$+43\overset{\circ}{.}53$
2013 12 04	$1^{\mathrm{h}}35.90^{\mathrm{m}}$	$+41\overset{\circ}{.}72$
2013 12 09	$1^{\mathrm{h}}26.33^{\mathrm{m}}$	$+39\overset{\circ}{.}89$
2013 12 14	$1^{\mathrm{h}}18.76^{\mathrm{m}}$	$+38\overset{\circ}{.}13$
2013 12 19	$1^{\mathrm{h}}12.99^{\mathrm{m}}$	$+36\overset{\circ}{.}46$
2013 12 24	$1^{\mathrm{h}}08.82^{\mathrm{m}}$	$+34\overset{\circ}{.}93$
2013 12 29	$1^{\mathrm{h}}06.06^{\mathrm{m}}$	$+33\overset{\circ}{.}55$
2014 01 08	$1^{\mathrm{h}}04.03^{\mathrm{m}}$	$+31\overset{\circ}{.}25$
2014 01 18	$1^{\mathrm{h}}05.68^{\mathrm{m}}$	$+29\overset{\circ}{.}54$
2014 01 28	$1^{\mathrm{h}}10.08^{\mathrm{m}}$	$+28\overset{\circ}{.}36$
2014 02 07	$1^{\mathrm{h}}16.55^{\mathrm{m}}$	$+27\overset{\circ}{.}62$
2014 03 01	$1^{\mathrm{h}}35.80^{\mathrm{m}}$	$+27\overset{\circ}{.}17$
2014 04 01	$2^{\mathrm{h}}10.01^{\mathrm{m}}$	$+28\overset{\circ}{.}27$
2014 05 01	$2^{\mathrm{h}}47.14^{\mathrm{m}}$	$+30\overset{\circ}{.}32$
2014 06 01	$3^{\mathrm{h}}26.92^{\mathrm{m}}$	$+32\overset{\circ}{.}85$
2014 07 01	$4^{\mathrm{h}}04.25^{\mathrm{m}}$	$+35\overset{\circ}{.}48$
2014 08 01	$4^{\mathrm{h}}37.57^{\mathrm{m}}$	$+38\overset{\circ}{.}50$
2014 09 01	$4^{\mathrm{h}}57.19^{\mathrm{m}}$	$+42\overset{\circ}{.}29$
2014 10 01	$4^{\mathrm{h}}44.41^{\mathrm{m}}$	$+47\overset{\circ}{.}10$
2014 11 01	$3^{\mathrm{h}}24.42^{\mathrm{m}}$	$+50\overset{\circ}{.}05$
2014 12 01	$1^{\mathrm{h}}43.26^{\mathrm{m}}$	$+42\overset{\circ}{.}90$
2015 01 01	$1^{\mathrm{h}}05.07^{\mathrm{m}}$	$+32\overset{\circ}{.}85$

Extended observations are needed for studying these phenomena and the dust particles involved. These will have a direct impact in the understanding of meteor producing meteoroids.

Some of the issues we have identified are:

a) Measuring the extent of the phenomena in time will provide information on solar radiation pressure on the particles and the particle size distribution.

b) Measuring the width of the hourglass center and inhomogeneity in the trail will quantify the expected non-regular radiation pressure effects, among these the seasonal type radiation effects.

c) Characterizing the brightness evolution of the trail(s). We expect this to provide information about the size-dependent evolution of the particles in the trail.

d) The observation of the hourglass center in February with similar observation in August may tell if the explosion was not symmetric in the radial direction.

e) To ascertain through study if a similar effect from the 1892/1893 eruptions (Sekanina, 2009) could still be observable.

Acknowledgements

The image subtraction was made with program Isis2.2 by Seppo Mattila, Tuorla Observatory, University of Turku.

Olli Lyytinen and Dr Ladan Cockshut provided proofreading assistance.

We thank the referees for helpful and constructive comments.

References

Alard C. (2000). "Image subtraction using a space-varying kernel". *Astronomy & Astrophysics Supplement*, **144**, 363–370.

Burns J. A. and Lamy P. L. (1979). "Radiation forces on small particles in the Solar System". *Icarus*, **40**, 1–47.

Fulle M. (2004). "Motion of cometary dust". In Festou M., Keller H. U., and Weaver H. A., editors, *Comets II*, pages 565–575. Univ. of Arizona Press.

IAU MPC (2013). "Elements and ephemeris for 17P/Holmes". `http://scully.cfa.harvard.edu/cgi-bin/returnprepeph.cgi?d=c&o=0017P` . (last visited 2013 May 10).

Ishiguro M., Watanabe J.-I., Sarugaku Y., Ootsubo T., Kuroda D., Honda M., Miyata T., Yanagisawa K., Mito H., Fukushima H., Niwa T., Sakamoto M., Narusawa S.-Y., and Akisawa H. (2010). "2007 outburst of 17P/Holmes: The albedo and the temperature of the dust grains". *Astrophysical Journal*, **714**, 1324–1333.

Lyytinen E. and Van Flandern T. (2000). "Predicting the strength of Leonid outbursts". *Earth, Moon, and Planets*, **82/83**, 149–166.

Lyytinen E., Van Flandern T., and Nissinen M. (2001). "Improved 2001 Leonid storm predictions from a refined model". *WGN, Journal of the International Meteor Organization*, **29**, 110–118.

Montalto M., Riffeser A., Hopp U., Wilke S., and Carraro G. (2008). "The comet 17P/Holmes 2007 outburst: the early motion of the outburst material". *Astronomy & Astrophysics*, **479**, L45–L49.

Sekanina Z. (2009). "Comet 17P/Holmes: A mega outburst survivor". *International Comet Quarterly*, **31**, 5–23. (`http://www.icq.eps.harvard.edu/ICQ-Jan-09-p5-23.pdf`).

Stevenson R. and Jewitt D. (2012). "Near-nucleus photometry of outbursting comet 17P/Holmes". *Astronomical Journal*, **144**, 138.

Suominen M. (2007). "Yllättäjä Holmes hohtaa tähtenä Perseuksessa". *Tähdet ja Avaruus*, **37:7**, 7. (Comet Holmes – the astonishingly shining star of Perseus, in Finnish).

Handling Editor: Jürgen Rendtel

NEMETODE: The Network for Meteor Triangulation and Orbit Determination. System Overview and Initial Results from a UK Video Meteor Network

William Stewart[1], *Alex R Pratt*[2] *and Leonard Entwisle*[3]

An overview is provided and first results presented from NEMETODE, The Network for Meteor Triangulation and Orbit Determination. This is a network of four low-light video cameras based in the North of England in the United Kingdom that use UFOCapture, UFOAnalyser and UFOOrbit to capture and analyse meteor data. NEMETODE is intended to supplement the increasing number of comparable teams around the world who are using similar networks. Many of these networks have been established to ascertain if the suspected meteor showers listed on the International Astronomical Union's Meteor Data Center actually exist and if so, determine if they can be associated with known parent bodies. This paper provides a detailed description of the equipment used and the techniques employed to collect and analyse the data. The results from the first full collaborative month of operation, 2012 August, are presented, with specific focus given to the 007 PER (Perseids) meteor shower. The Perseids are a well characterised shower and were selected to verify if the results from NEMETODE were consistent with currently accepted parameters.

Received 2013 January 29

1 Introduction

Using a network of cameras to simultaneously record the same meteor event from different geographical locations offers a number of advantages. Specifically the meteoroid's trajectory through the Earth's atmosphere can be triangulated, thus allowing characteristics such as the radiant and the beginning / end heights to be determined. Combining this information with timing data (when the event occurred, angular speed across the Field of View (FOV)) permits an estimate to be made of the meteoroid's original orbit around the Sun. From this an association may be made with a parent body. This is discussed elsewhere in greater detail (Jenniskens et al., 2011) and does not warrant further discussion here.

2 Network Overview

NEMETODE consists of three stations or nodes. The first is operated by William Stewart (WS) and is located in Ravensmoor, near Nantwich, Cheshire. The second is operated by Alex R Pratt (ARP) and is located in Leeds, West Yorkshire while the third is operated by Leonard Entwisle (LE) from Elland, West Yorkshire.

2.1 Ravensmoor Node

The Ravensmoor Node operates two similar camera systems. The cameras are Watec 902H units (1/2" sensor) coupled with Computar 8 mm $f/0.8$ lenses. The North facing camera has a Computar HG0808AFCS-HSP lens while the East facing camera has a HG0808FCS-HSP lens. Each yields a resolution of 3.63 arcmin per pixel. The instructions for this lens call for the supplied "B/W Aberration Compensation Filter" to be fitted between the lens and the camera but in the case of the Watec 902H, this is not possible as the filter touches the inside of the camera body before the threads on the rear of the lens are able to engage with those on the camera. Attempting to use a C/CS Mount adapter ring (which increases the distance between the lens and camera by 5 mm) allows the filter to be fitted. However when this is done it is no longer possible to focus the lens at infinity – as a result the filter is not fitted.

The lens has an auto-iris that, by default, is closed. The Watec 902H does not support auto-iris lenses so the Ravensmoor cameras operate with the iris opened fully by applying a voltage of 12 V DC across the red (+ve) and black (−ve) leads. The white lead is not required.

Focus is achieved by rotating the barrel of the lens. There is a screw that can be tightened to lock the focus position but repeated heating / cooling (hot days and cold nights) can result in the screw becoming loose and the focus drifting. A length of adhesive tape has therefore been affixed around the lens barrel to hold each focus ring in position.

Each camera is located in its own Closed Circuit Television (CCTV) Housing affixed to the gable end of a brick building (see Figure 1). The housings are weatherproof, have heated glass front windows and sufficient internal space for ease of fitting of / access to the cameras. Pointing and FOV details are as follows:

Ravensmoor	North	East
Azimuth (centre)	$18.^\circ5$	$90.^\circ8$
Elevation (centre)	$48.^\circ9$	$46.^\circ8$
Field of View	$43.^\circ5$ (H) × $33.^\circ3$ (V)	

The camera, iris on the lens and the heater on the CCTV housings all operate at 12 V DC. Laptop style power supplies were initially used to convert 230 V AC to 12 V DC but these were susceptible to intermittent problems with banding on the videos and images. The problem was traced to the push-fit electrical connections. Slightly twisting them temporarily cured the problem but it always came back after a few days. Replacements that made use of screw terminals (as opposed to the problematic push fit connectors) were required but during the specification phase it was deter-

[1]Email: ws@nemetode.org
[2]Email: arp@nemetode.org
[3]Email: le@nemetode.org

IMO bibcode WGN-413-stewart-nemetode
NASA-ADS bibcode 2013JIMO...41...84S

Figure 1 – Both cameras of the Ravensmoor Node permanently affixed to the gable end of a brick building. The unit on the left faces east while that on the right faces north. Note the black spacer block on the left hand unit between the camera housing and the mounting bracket. This modification was required in order to allow the appropriate elevation to be achieved without the rear of the housing fouling on the horizontal support bracket.

mined that a power supply that provided enough current to drive additional systems (for future expansion) would be desirable. A Sunpower 60 W 12 V DC 5 A Single Output AC-DC Enclosed Power Supply was selected and installed. This power supply is passively cooled and so no cooling fans are required.

All of the power is linked together, i.e. the power for the camera, iris on the lens and the heater on the CCTV housing all come from the same source (the power supply described above) and switch on / off together. Some meteor detection networks recommend having separate power supplies for the camera and the heater in order to avoid the potential of introducing noise to the system when the heater switches on and off. The Ravensmoor system has, as noted above, a common power supply and has not experienced any such switching issues.

In order to protect the camera and lens from damage, it is essential that the iris on the lens is closed and the camera powered off during daylight hours, particularly as one of the cameras is east facing. Direct sunlight falling on the fully operational system will quickly damage the sensor. Initially a simple rotary time-switch with the settings corresponding to the hours of nautical twilight was used. The times of nautical twilight can be easily determined for the observer's particular location by using the website of the US Naval Observatory.[1] This website allows the user to choose between civil, nautical and astronomical twilight. Settings for nautical twilight were initially chosen as this seemed to be the best compromise between not too bright to risk damage to the system and dark enough that there was the possibility of detecting a meteor. However two problems became apparent:

i. The settings on the rotary time-switch had to be regularly altered, particularly at times close to the equinox when the start / end of nautical twilight changed rapidly from one day to the next.

ii. As the power for the heater on the CCTV housing was activating at the same time as the camera and iris on the lens, initial video images were not good on occasions when there was condensation on the glass window at the front of the CCTV Housing – it took a few minutes for the heater to clear the condensation.

Images taken at sunset / sunrise were not saturating the sensor (the "shutter" switch on the rear of the Watec 902H camera is set to the "on" position) and so WS decided to have the switch activation coincide with sunrise and sunset. Although the sky would be too bright to detect meteors, it would give time for the heater to do its job and clear any condensation before the sky became dark enough for meteors to become visible.

The best solution found was to make use of a Theben SEL170 time-switch. This self contained device is able to switch 240 V AC, takes account of the observer's location and date and automatically adjusts the on / off times based on local sunset / sunrise times that it itself calculates. This solution has now been implemented at the Ravensmoor node and controls the power to all cameras, lenses and heaters.

Each camera is connected to its own dedicated desktop PC. A desktop was chosen as they are relatively inexpensive, powerful for the price, easy to repair and upgrade, have enough slots for extra RAM and space for additional Hard Disk Drives (HDDs). IBM M51 3.2 GHz P4 HT models were selected and upgraded from the standard specification to ones with 2 GB RAM and an additional 250 GB HDD. Under normal operation (resolution 762×576, 25 frames per second (fps)), the CPU load is in the region of 17 – 18%. The Operating System is Windows XP. The following lessons were learnt during the commissioning phase:

i. Disable HDD Power Saving. This can be done through the BIOS and / or via the Power Options menu in Windows. When a meteor is detected, the PC will need to transfer significant amounts of data from the memory buffer to the HDD in a very short period of time, while at the same time read (and monitor) the ongoing live video stream into the memory buffer. Prior to disabling the HDD Power Saving feature it was found that after a period of inactivity, frames were being lost from video clips while the HDD spun up from the auto powered down state.

ii. A reasonable size HDD (>100 GB) dedicated to the data (i.e. separate from the main HDD for the Operating System (OS)) avoids issues with the PC being occupied with normal OS issues when it needs to write video data. It also avoids the need for regular data transfer from one HDD to an archive. A minimum of 30 GB space is kept free at all times and the disk is regularly defragmented (circa once per week) – again, video frames can be dropped if the HDD Read / Write Head has to execute significant movements between sectors when writing to the disk. During nights of exceptionally poor seeing the detection software can

[1] `http://aa.usno.navy.mil/data`

interpret excessive scintillation as movement that should be recorded – some videos can then become a few minutes (as opposed to a few seconds) long, thus consuming considerable HDD space. UFOCapture provides the user with extensive tuning capabilities to minimise such occurrences but the preference amongst the NEMETODE members is to have the detection threshold as low as possible in order to reduce the likelihood of a missed meteor.

iii. Set the PC time to GMT and disable the "Automatically Adjust to Daylight Savings Time" feature. The timestamps for each file will then always be in UTC and won't suddenly jump by one hour twice per year when daylight savings starts / finishes. This is particularly useful when checking if the same event has been captured by another system – data-files can be compared automatically without the need for manual tweaking.

iv. The timestamp for each file is based on the PC's internal clock. This can drift by varying amounts each day and as a consequence each PC is set to auto-synchronise with an internet time server every 15 minutes using Dimension 4 software.[2] Typical corrections are of the order of 10–20 ms. Without this application running, the PC's internal clock would lose approximately 10 s every week. The aforementioned software is able to generate a text file that provides details of the timing corrections that have been applied to the PC's internal clock. This data is reviewed prior to each analysis to ascertain if large (>0.5 s) changes occurred during observing runs (and could therefore potentially affect the timing data). A review also helps highlight if there are avoidable scheduling issues (for example regular data uploads / downloads that could negatively impact bandwidth availability).

v. When running more than one system from the same internet connection, it is worth monitoring when the synchronisations occur. Sometimes they can end up simultaneously requesting a timing correction (for example if the internet connection goes down and then becomes available again, perhaps due to a power outage or maintenance work). For autonomous operation one can reduce the impact of this issue by having each PC synchronise after a different number of set minutes.

vi Auto-synching the PC clock does require a permanent internet connection. The Ravensmoor systems use AVG Free as a firewall and Malware Bytes for additional protection.

vii Ensure that security updates and scans using these or other programs, together with any Windows Updates, are scheduled for daylight hours when the PC will not be busy detecting meteors. It is also important to set the Windows security settings to not automatically install updates as these can, at times, trigger an auto-restart of the PC. It has also been found to be beneficial to restart the PC every so often, again during daylight hours, just to ensure that any cumulative memory issues don't lead to problems during the observing runs. For the Ravensmoor systems this is performed once per week.

viii Overall PC maintenance is essential and so it is important to monitor air inlets for the computer and vacuum them clean when they become dusty – if the PC runs 24 hours per day / 7 days per week then it may overheat and crash / lockup during warm weather. Keeping the cables at the rear of the PC neatly bundled away from the exhaust vents also helps with the airflow.

The initial selection of video cards to accept the signal from the cameras resulted in less than ideal performance. While they worked most of the time, a significant number of frames were being dropped. WS is indebted to Robert Cobain (Cobain, 2005) who operates a dual station meteor detection system in conjunction with Armagh Observatory in Northern Ireland (Armagh Observatory, 2009) for his recommendation to use an Osprey 210 Video Card. While these are slightly more expensive than other cards, they do have excellent performance characteristics and since switching to this card the system has worked perfectly.

The cable run from each camera to each PC is of the order of 10 m. Initially a combined video / power cable solution was implemented but this proved short-lived as part of the cable run is outside and is therefore exposed to the elements. The cable failed after a few months as repeated exposure to frost snapped the very fine inner cores of the power lead. The combined lead was replaced with separate dedicated lines for power and video. A double shielded RCA video lead (one with a central core, copper braid and a foil sheath) was selected both for its robustness (thicker wires) and in order to reduce the amount of noise on the video signal. The two core power lead has an exterior grade sleeve to protect it from the elements.

The whole system (PC, camera, iris on the lens, heater on the CCTV housing) all operate off an Uninterruptable Power Supply (UPS) so that in the event the mains power is interrupted, the system will continue to operate for up to 30 minutes. The system is located in an area that was prone to intermittent power outages lasting a second or two – just long enough to crash the PC. It should however be noted that since the investment in and the installation of the UPS, the local power lines have been replaced and the frequency of power outages has decreased from once per week to less than once per year.

The systems are very sensitive – on a clear, moonless night they are each capable of detecting, in real time, stars down to better than magnitude +5.5 though in practice the system struggles to detect meteors fainter than magnitude +4.

While UFOCapture does have excellent configurable settings to reduce the likelihood of non-meteor events resulting in a clip, some do on occasion slip

[2] `http://www.thinkman.com/dimension4`

through. Depending on the time of year and local lighting conditions, these can include birds, bats, insects, firework flashes, snowflakes, falling leaves and of course aeroplanes and satellites. On a regular basis (typically daily) the video clips from the previous night are reviewed and unwanted clips deleted. The data is copied to separate hard-drives for analysis and backup.

2.2 Leeds Node

The Leeds node operates a South-facing Watec 902H2 Ultimate camera (1/2" sensor) with a Computar HG3808 FCS-HSP 3.8 mm $f/0.8$ lens and B/W Aberration Compensation Filter, giving a resolution of 6.63 arcmin per pixel. The auto-iris is driven by the camera.

The camera and lens (and a large bag of silica desiccant gel) reside in the same model of CCTV housing as used by the Ravensmoor node. It is mounted on the southwest corner of the house. Pointing and FOV details are as follows:

Leeds	
Azimuth (centre)	$184\overset{\circ}{.}3$
Elevation (centre)	$49\overset{\circ}{.}8$
Field of View	$89\overset{\circ}{.}2$ (H) $\times 68\overset{\circ}{.}6$ (V)

The camera and heater are powered by separate 12 V DC mains adapters. They are not triggered by a self-timer, so ARP manually switches them on / off at dusk / dawn. The Leeds system has not (yet) had problems with condensation so the heater is rarely switched on.

The Leeds node uses a dedicated tower PC, a Dell Dimension DXP061 running under Windows Vista Home Premium, with dual Intel 2.13 GHz CPUs, 4 GB RAM and a 300 GB HDD. The disk is defragmented every week and a separate HDD has not been necessary. Anti-Virus and Firewall protection are provided by Norton's software. Automatic Windows Updates are disabled, then checked manually and applied during the day.

As with the Ravensmoor node the Windows setting for HDD Power Saving was disabled. The PC was synchronised once per evening with an Internet time service. Some of the Perseids captures had to be time-corrected, using the method described in Section 3.1. Commencing 2012 October the PC is (just like at Ravensmoor) synchronised every 15 minutes with an NTP time server using Dimension 4 software.

Video capture is performed by a USB 2.0 device from ClimaxDigital and in normal operation (resolution 720×576, 25 fps), the CPU load is about 20%. The cable run is also 10 m, with a combined power/video cable for the camera and a separate cable for the heater. The cables have not caused any problems. Power cuts are very rare for the Leeds node so a UPS is not required although the equipment is connected to a mains surge protector.

The city sky is light-polluted with a video limiting magnitude of about +3.5. Captures often include many aeroplanes, so unwanted videos are deleted each day. Data backups are saved to external drives and to another PC on which the analyses are performed.

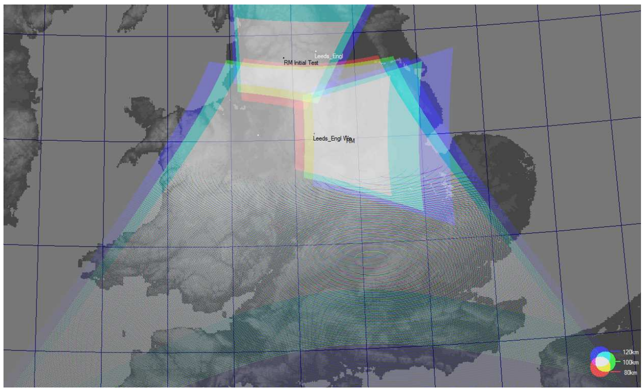

Figure 2 – Field of View (FOV) coverage of the NEMETODE cameras for Leeds and Ravensmoor for the period 2012 July – December. The different colours represent different altitudes. The red represents 80 km, the light blue 100 km and the dark blue 120 km. The almost transparent white is where there is single station coverage of a layer between 80 km and 120 km while the almost opaque white is where there is dual station coverage of a layer between 80 km and 120 km. While this shows the FOV, other factors such as local weather and the effects of atmospheric extinction limit the range over which meteors are detected

2.3 Elland Node

The Elland node is not a UFOCapture station. LE occasionally runs a tripod-mounted Watec 902H camera with an aspherical Computar 3.8 mm $f/0.8$ lens, facing South. Recordings are made to VHS tapes, with a manually synchronised time-and-date inserter. The video limiting magnitude is +3.

2.4 Overall Coverage

NEMETODE was created after an exchange of comments on a meteor forum relating to a fireball event that occurred over northern England at 2012 July 28, $00^h58^m47^s$ UT. While ARP and LE were aware of each other's work, they were not aware of WS's setup, or he of theirs. Following discussion of the July fireball it was realised that, fortuitously, the same volume of atmosphere was being monitored by different cameras and that as a consequence, triangulation could be performed using SonotaCo's UFOOrbit program.

The baseline between Leeds and Elland is relatively short (21 km) but between Leeds and Ravensmoor it is 107 km – a distance that is much more effective for triangulation work. Figure 2 shows the coverage plot for Ravensmoor and Leeds. It was obvious from the outset that overall coverage could be improved through simply re-aligning some of the cameras. However ARP and WS decided to leave their cameras on their original elevation / azimuth settings for the remainder of 2012 in order to ascertain the quality of data from their existing setups. As of the time of writing (2013 January) this initial commissioning phase has been completed and the cameras have been re-aligned and augmented with an additional camera in order to maximise dual station coverage. Further details of this enhanced coverage are available on the authors' website `http://www.nemetode.org`.

2.5 Software

The data from all NEMETODE nodes is captured and analysed using SonotaCo's UFO Suite. In addition, a number of custom spreadsheets are used to analyse timing corrections to the PC's internal clock, to provide an independent check of concurrence of event start times and to perform orbital parameter analysis.

3 Data Analysis

Members of NEMETODE adopt the same consistent approach when analysing their data and complete a shared checklist to minimise variation. Although UFOAnalyser has automated functionality for data reduction, the NEMETODE team has found that in a few cases (<10%), the assigned meteor trajectory is slightly misaligned but can be corrected by adjusting a number of software parameters as described in the UFOAnalyser manual. As a result the NEMETODE team perform a series of manual checks for each event.

3.1 Analysis Methodology

For each event the following checks are applied:

i. Timing corrections that have been applied to the PC's internal clock are reviewed to ascertain if there is an error of >1.0 s in any of the timestamps associated with each video clip.

ii. The SonotaCo BBS Forum[3] is checked to verify if there are any software updates that need to be applied (e.g. updated software versions, leap second corrections).

iii. The assigned stellar background for a given profile is checked to ensure it is a good match for the stars visible in the composite image. If not, a new profile is generated.

iv. Each clip is reviewed to ensure the meteor commences within 1.0 s of the time-stamp assigned to the video clip.

v. The assigned meteor trajectory is checked to ensure it is a good match for the meteor trail on the composite image. If not, adjustments are made to the appropriate settings within the UFOAnalyser software (as detailed in the user manual) and the analysis re-performed until a good match is obtained.

As can be seen from Section 3.1 points (i.) and (iv.) there are occasions when the time-stamp attributed to an event may be incorrect. Examples of this include the PC Clock being incorrect or a video clip is triggered by a non-meteor event (e.g. excessive stellar scintillation or an aeroplane enters the FOV) but a meteor does subsequently appear and is recorded within the video clip. Under these circumstances, a timing correction needs to be applied and the following process is followed:

[3] http://sonotaco.jp/forum/viewforum.php?f=17

i. A copy of the original M.XML file (which contains details of the start time of the meteor event) is saved in a secure location (for archival purposes).

ii. The frames of the video clip are stepped through one at a time until the first evidence of the meteor appears. The start time of the meteor (from the time code at the bottom of the frame) ±0.1 s is noted.

iii. The original M.XML file (not the copied version) is edited to give the start time of the meteor noted in step ii. above.

iv. If it already exists (from a previous analysis), the MA.XML file is deleted.

v. UFOAnalyser is re-run for this particular video clip using the updated M.XML file.

vi. The new M.CSV file is saved and verification that the correct meteor start time has been written to the MA.XML and M.CSV files is performed (note that the filenames will remain unchanged and will still show the original start time of the video clip).

In a typical month each camera of the NEMETODE network will record a minimum of 100 meteors (often more, depending on shower season and weather) and so while this level of diligence may seem onerous, the authors feel it is essential in order to maximise the data-set with which further analysis can be reliably performed.

The resultant M.CSV files are then emailed between the members of the NEMETODE team. As an additional check however, the data is also compared in a custom spreadsheet to ascertain how many events have a common start time (±1.0 s) and thus may be different captures of the same event.

The data then undergoes an initial analysis using UFOOrbit and the number of events compared against the aforementioned spreadsheet. Any discrepancies are investigated and dispositioned at this stage and the spreadsheet that tracks the efficiency of NEMETODE network updated. A more detailed analysis is then performed.

3.2 Perseids Analysis

3.2.1 Preamble

The first likely Perseid candidate was recorded at Leeds on 2012 July 12, $01^h24^m56^s$ UT and the last on 2012 September 11, $23^h06^m20^s$ UT, again at Leeds. The magnitude distribution from 2012 July 11 to September 12 (measured by UFOAnalyser) is given in Table 1 (meteors from minor showers are not included). The activity profile of the Perseids is presented in the graph in Figure 3 (All dates are $00^h00^m00^s$ UT).

3.2.2 Multi-station Perseid Meteors

UFOOrbit provides three built-in Quality Assurance criteria:

Q1: minimum criteria for radiant computation; Q2: standard criteria for radiant and velocity computation; Q3: criteria for high precision computation.

Table 1 – Magnitude distribution of Perseid and sporadic meteors.

	−4	−3	−2	−1	0	+1	+2	+3	+4	Mean
Leeds										
Perseids	0	3	14	47	63	31	1	0	0	−0.3
Sporadics	1	3	11	25	38	20	0	0	0	−0.4
Ravensmoor East										
Perseids	2	3	13	38	56	23	0	0	0	−0.4
Sporadics	0	2	7	32	81	63	4	0	0	+0.1
Ravensmoor North										
Perseids	0	3	3	9	21	43	78	16	1	+1.3
Sporadics	0	1	2	13	21	71	96	18	0	+1.3

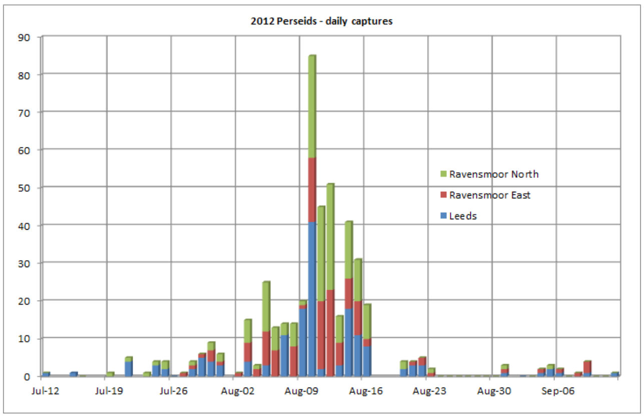

Figure 3 – Daily Perseid Video Captures. The histogram indicates that Perseid rates were low until there was a small increase around 2012 July 20/21. Activity picked up after 2012 August 04/05, with peak activity between 2012 August 08/09 to 13/14, although bad weather hampered observations on the nights of maximum. Rates declined rapidly after 2012 August 15/16. The activity profile is generally symmetrical, with a suggestion that it is skewed to the left.

Note that when grouping captures, Q1 includes level Q2 and Q3 data, Q2 includes level Q3 data.

Between 2012 July 30 and September 03 a total of 40 Q1 multi-station Perseids were captured by ARP and WS. ARP post-processed LE's tapes from the nights of 2012 August 08/09 and 09/10 via UFOCapture and UFOAnalyser but could not obtain an average star alignment error < 1.0 pixel (the UFOAnalyser Manual recommends a figure of <0.3 pixel). Almost all of the data were rejected at the Q1 level, except for a Perseid on 2012 August 08 at $23^{\mathrm{h}}07^{\mathrm{m}}43^{\mathrm{s}}$ UT, which is a tri-station capture. The ground tracks of the 40 Q1 multi-station Perseids (derived by UFOOrbit) are shown in Figure 4.

3.2.3 Radiant Drift

UFOOrbit was used to derive the radiant point for each multi-station Perseid, corrected for Zenith Attraction. The positions of the radiant points from 40 multi-station Perseid meteors between 2012 July 30 and September 03 were used to estimate the daily drift of the radiant in Right Ascension and Declination and the results are plotted in Figure 5.

3.2.4 Radiant drift in Right Ascension

The method of least squares gives a good linear fit:

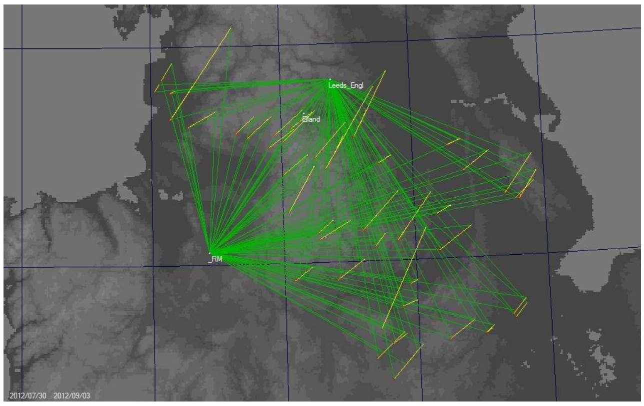

Figure 4 – Ground tracks of 40 Q1 Perseid meteors.

$$\alpha = 1.285 \times \lambda_\odot - 131\overset{\circ}{.}56 \quad (r = 0.937) \qquad (1)$$

The daily motion in RA during the observed period is estimated as $1\overset{\circ}{.}29$, which is close to the value of $1\overset{\circ}{.}35$ by Cook (1973) quoted in the 2012 British Astronomical Association (BAA) Handbook.

If the Perseid maximum occurred at solar longitude $140\overset{\circ}{.}0$ the estimated RA at maximum is $\alpha = 48\overset{\circ}{.}3$ ($3^{\mathrm{h}}13^{\mathrm{m}}$), as presented in Table 2.

3.2.5 Radiant drift in Declination

The method of least squares gives the linear fit:

$$\delta = 0.209 \times \lambda_\odot + 28\overset{\circ}{.}67 \quad (r = 0.576) \qquad (2)$$

There is a lot of scatter in the data, showing weak correlation, but the daily motion in Declination during the observed period is estimated as $0\overset{\circ}{.}21$, which is not too dissimilar from the value of $0\overset{\circ}{.}12$ by Cook (1973) quoted in the 2012 BAA Handbook.

If the Perseid maximum occurred at solar longitude $140\overset{\circ}{.}0$ the estimated Declination at maximum is $\delta = 57\overset{\circ}{.}9$, as presented in Table 2.

Table 2 – The Right Ascension and Declination of the Perseid radiant at maximum, and their geocentric velocities.

	$\lambda_\odot$	RA [°]	Dec [°]	v_g [km/s]
ARP/WS/LE	140.0	48.3	57.9	59.1
BAA	139.9	46	58	—
IAU MDC	140.19	48.33	57.96	59.38
IMO	140.0–140.1	48	58	59

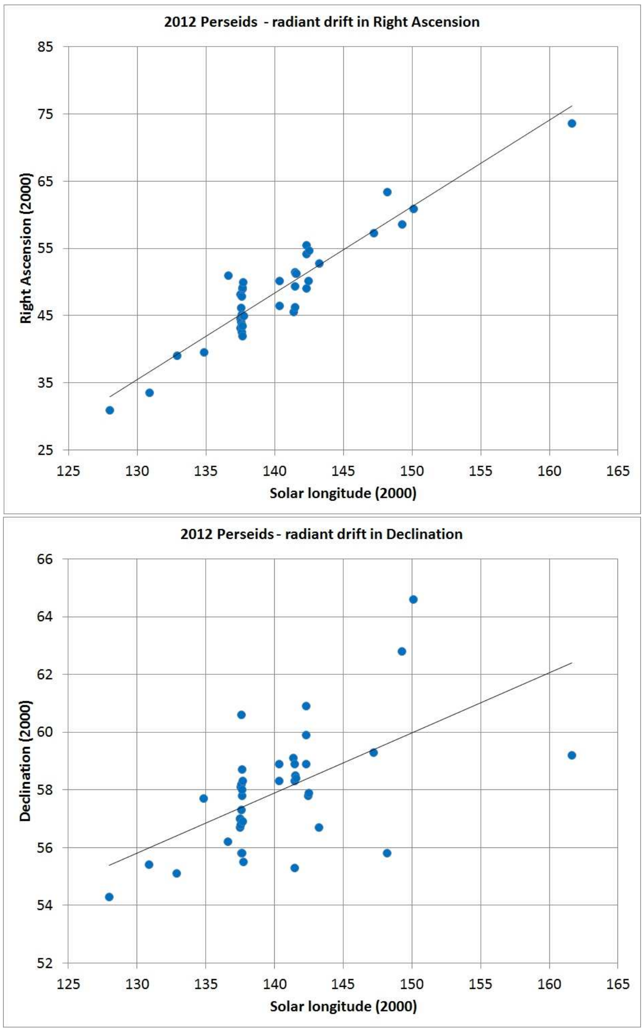

Figure 5 – Radiant drift in Right Ascension (top) and in Declination (bottom).

3.2.6 Meteor detection and extinction altitudes

UFOOrbit computed the start and end heights of 15 Q2 Perseid meteors, captured between 2012 July 30 and August 15 (see Figure 6). The method of least squares gives the linear fits:

$$h_b = 1.29 \times M + 113.0 \quad r = 0.447 \tag{3}$$

$$h_e = 4.24 \times M + 99.3 \quad r = 0.785 \tag{4}$$

where h_b is detection altitude, h_e is extinction altitude and M is absolute magnitude.

This suggests that Perseids burn up about 4 km lower in altitude for every 1 magnitude increase in brightness.

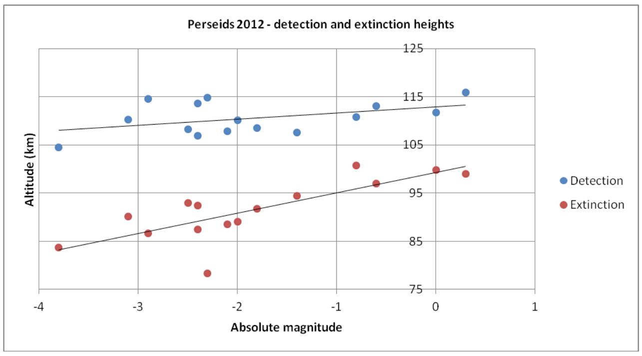

Figure 6 – Detection and extinction heights of 15 Q2 Perseid meteors.

3.2.7 Geocentric velocities

UFOOrbit computed the geocentric velocities, v_g, of the 15 Q2 Perseid meteors, which gave the following: $v_g = 59.1 \pm 0.96$ km/s. This compares well with the International Astronomical Union's Meteor Data Center (hereafter referred to as IAU MDC)[4] and IMO (McBeath, 2011) data (see Table 2).

3.2.8 Orbits of Perseid meteors

UFOOrbit computed the orbital elements of 6 Q3 Perseids. For each pair of observations it calculated 2 orbits and a Unified orbit. Key Characteristics of the Unified orbits are given in Table 3 while Figure 7 displays the "Top" view of the orbits.

3.2.9 Conclusions

The results derived from the video observations of the Perseids meteors by NEMETODE are consistent with the shower data catalogued by the BAA, IAU MDC and IMO. By applying Quality Assurance checks the authors now have confidence that NEMETODE equipment and methods should give reliable results for other meteor showers.

There is some variability in the Perseid orbital elements, especially the estimates of the semi-major axis a and period P, presented in Table 3. The authors' value of a is significantly different from that quoted by the IAU MDC and is nearer to the value of the Perseids' parent comet 109P/Swift-Tuttle (JPL SSD, 2013). A small error in the measured position and estimated geocentric velocity can give larger errors in the values of the orbital parameters a and P. As shown in Table 1, the

[4] `http://www.astro.amu.edu.pl/~jopek/MDC2007/`

Table 3 – Orbital parameters of 6 Perseid meteors with IAU MDC shower data shown for comparison.

$\lambda_\odot$	a (AU)	q (AU)	e	P (year)	ω (°)	Ω (°)	i (°)
137.5025	17.0	0.951	0.944	70.383	150.7	137.50	114.16
137.5710	15.6	0.941	0.940	61.581	148.3	137.57	114.10
137.6279	11.1	0.941	0.916	37.170	148.2	137.63	107.48
137.6401	37.0	0.958	0.974	224.789	152.8	137.64	112.15
137.7316	8.2	0.950	0.884	23.522	150.0	137.73	115.86
142.4478	14.3	0.958	0.933	53.829	152.7	142.45	114.38
Mean	17.2	0.950	0.932	78.545	150.5	138.42	113.02
Std. dev.	10.2	0.008	0.030	73.610	2.0	1.98	2.96
IAU MDC	71.4	0.953			151.3	140.19	113.22

authors' equipment is limited to detecting bright multi-station meteors (brighter than magnitude +2.0) so we are only monitoring and analysing a restricted sample of the meteor shower. SonotaCo (pers. comm., 2012) has confirmed that orbital analysis of meteors with high geocentric velocities is at the limits of the current equipment and it is anticipated that better results will be obtained from showers with relatively slower meteors.

References

Armagh Observatory (2009). "Automatic meteor detection system". http://star.arm.ac.uk/meteor-cam/ .

Cobain R. (2005). "Setting up a meteor observing station by Robert Cobain". http://www.eaas.co.uk/cms/index.php?option=com_content&view=article&id=69:setting-up-a-meteor-observing-station-by-robert-cobain-&catid=10:equipment-reviews&Itemid=16 .

Cook A. F. (1973). "A working list of meteor streams". In *Evolutionary and Physical Properties of Meteoroids*. pages 183–191. NASA SP-319.

Jenniskens P., Gural P., Dynneson L., Grigsby B., Newman K., Borden M., Koop M., and Holman D. (2011). "CAMS: Cameras for Allsky Meteor Surveillance to establish minor meteor showers". *Icarus*, **216**, 40–61.

JPL SSD (2013). "109P/Swift-Tuttle". http://ssd.jpl.nasa.gov/sbdb.cgi?sstr=109P .

McBeath A. (2011). "IMO 2012 Meteor Shower Calendar". IMO_INFO(2-11).

Handling Editor: Javor Kac

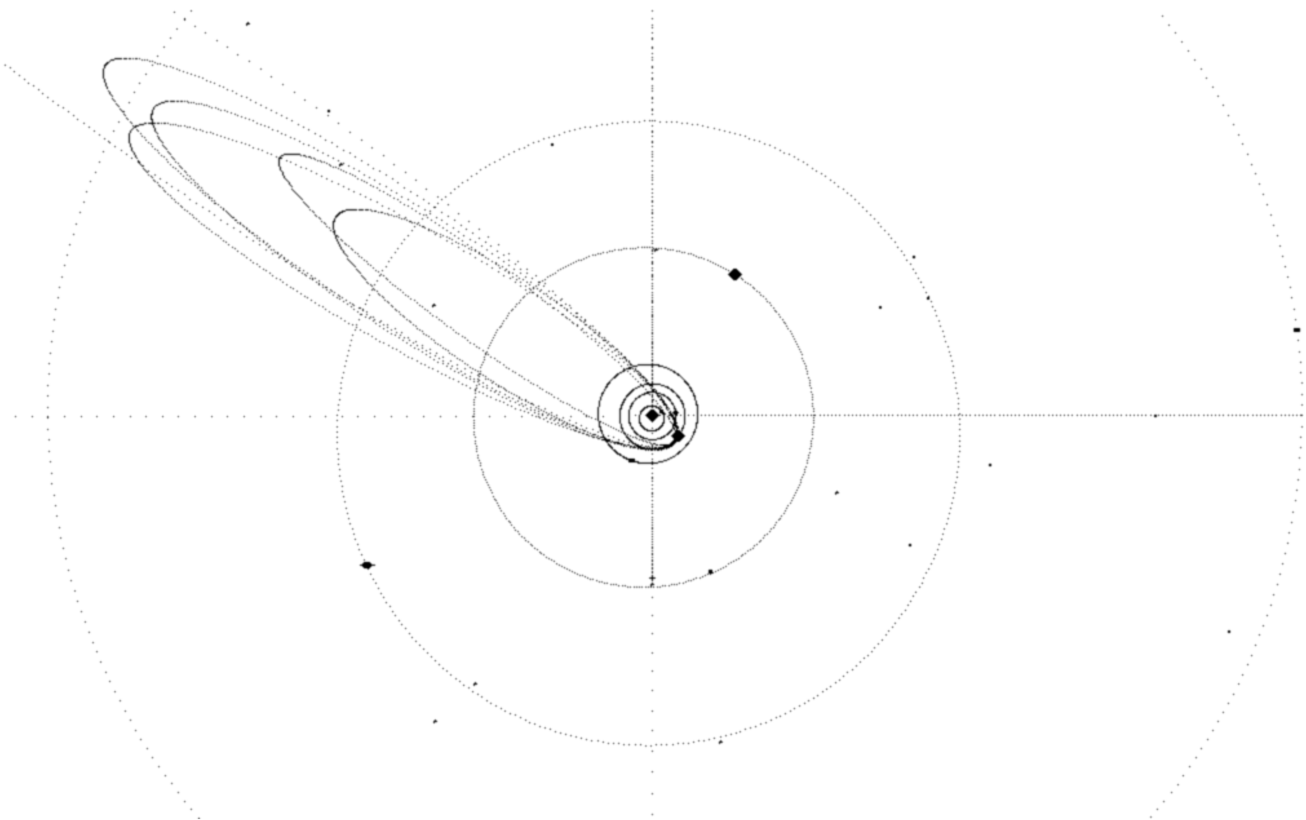

Figure 7 – "Top" view of the computed orbits of the 6 Q3 Perseid meteors.

Preliminary results

Results of the IMO Video Meteor Network — February 2013

Sirko Molau[1], *Javor Kac*[2], *Erno Berko*[3], *Stefano Crivello*[4], *Enrico Stomeo*[5], *Antal Igaz*[6], *Geert Barentsen*[7] *and Rui Goncalves*[8]

The February 2013 report of the IMO Video Meteor Network is presented, based on almost 10 000 meteors recorded by 67 cameras in about 4 800 hours of observing time. Shower parameters for the β-Herculids, Antihelion source and February η-Draconids are presented.

Received 2013 April 18

1 Introduction

With respect to the observing conditions, January 2013 was catastrophic, but February was not any better. There were hardly any starry nights in central and eastern Europe, and even our observers in Italy and at the Iberian peninsula had to step back a bit. In addition, a number of cameras were out of order or under reconstruction. Only seven of the overall 67 cameras obtained twenty or more observing nights for 2013 February. Compared to 2012, the effective observing time fell by 40% to about 4 800 hours (Table 5 and Figure 1). For the first time in the last two and a half years we recorded fewer than 10 000 meteors in a month, unless the missing 32 meteors are reported late. Also that figure for total meteors is 40% smaller than last February (Molau et al., 2012).

In addition to the unfavorable weather conditions, February is poor in meteor showers – perhaps the month with fewest meteor showers of all. Whereas in January we could detect 11 meteor showers, our long-term analysis from spring 2012 (Molau, 2012) revealed only one shower in February with the typical criteria (activity in at least five degrees solar longitude), besides the Antihelion source.

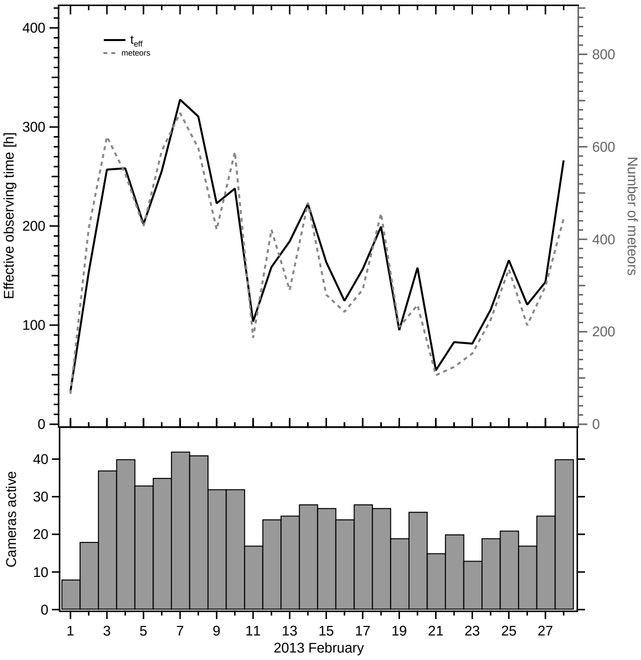

Figure 1 – Monthly summary for the effective observing time (solid black line), number of meteors (dashed gray line) and number of cameras active (bars) in 2013 February.

2 β-Herculids

The β-Herculids (418 BHE) are weak, but still detectable. Between February 13 and 16, the shower is continuously among the five strongest meteor sources in the sky and reaches a rank of four, at maximum. Roughly 150 meteors are assigned to that shower. There is good agreement with the MDC list values (Table 1), which is not really surprising given that the β-Herculids were detected in our own 2009 analysis, the data set of which was a subset on the new analysis. Only the sign of the radiant drift has changed, but that also is acceptable. If the activity interval is so short and if so few meteors are available, only minor changes in the radiant position or interval length can lead to different drift values.

3 Antihelion meteors

More prominent (with 1 500 meteors in our database) is another shower in February, which is detected between January 26 and March 4. Most of the time it is the strongest source in the night sky. The scatter in meteor shower parameters is acceptable and the activity profile is flat with no structure. Our analysis software identified this shower as the Northern δ-Leonids (112 NDL), but our radiant is almost ten degrees away from the position given in the MDC list, and also the velocity deviates significantly. Thus, the meteor shower assignment is questionable. The shower is a much better fit to the Antihelion source, which lies at the ecliptic about 15° east of the antihelion point (Table 2).

[1]Abenstalstr. 13b, 84072 Seysdorf, Germany. Email: sirko@molau.de
[2]Na Ajdov hrib 24, 2310 Slovenska Bistrica, Slovenia. Email: javor.kac@orion-drustvo.si
[3]Bercsenyi ut 3, 3188 Ludanyhalaszi, Hungary. Email: berkoerno@invitel.hu
[4]Via Bobbio 9a/18, 16137 Genova, Italy. Email: stefano.crivello@libero.it
[5]via Umbria 21/d, 30037 Scorze (VE), Italy. Email: stom@iol.it
[6]Húr u. 9/D, H-1223 Budapest, Hungary. Email: antaligaz@yahoo.com
[7]University of Hertfordshire, Hatfield AL10 9AB, United Kingdom. Email: geert@barentsen.be
[8]Urbanizacao da Boavista, Lote 46, Linhaceira, 2305-114 Asseiceira, Tomar, Portugal. Email: rui.goncalves@ipt.pt

IMO bibcode WGN-413-molau-vidfeb
NASA-ADS bibcode 2013JIMO...41...92M

Table 1 – Parameters of the β-Herculids from the MDC Working List and the analysis of the IMO Network in 2012.

Source	Solar Longitude		Right Ascension		Declination		v_∞	
	Mean [°]	Interval [°]	Mean [°]	Drift [°]	Mean [°]	Drift [°]	Mean [km/s]	Drift [km/s]
MDC	324	322-326	246.0	+0.9	+23.5	−0.9	55.5	—
IMO 2012	325	324–327	246.4	−0.9	+24.9	+1.2	54.3	—

Table 2 – Parameters of the Antihelion source in February from the analysis of the IMO Network in 2012.

Source	Solar Longitude		Right Ascension		Declination		v_∞	
	Mean [°]	Interval [°]	Mean [°]	Drift [°]	Mean [°]	Drift [°]	Mean [km/s]	Drift [km/s]
—	325	—	157	—	+7.8	—	30	—
IMO 2012	325	306–343	157.2	+1.0	+10.2	−0.3	29.3	—

Table 3 – Parameters of the February η-Draconids from the MDC Working List and the analysis of the IMO Network in 2012.

Source	Solar Longitude		Right Ascension		Declination		v_∞	
	Mean [°]	Interval [°]	Mean [°]	Drift [°]	Mean [°]	Drift [°]	Mean [km/s]	Drift [km/s]
MDC	315.1	—	239.6	—	+62.5	—	37.3	—
IMO 2012	315	314–317	239.9	+0.5	+60.9	−0.1	33.8	—

Table 4 – Parameters of a possibly unknown meteor shower from the analysis of the IMO Network in 2012.

Source	Solar Longitude		Right Ascension		Declination		v_∞	
	Mean [°]	Interval [°]	Mean [°]	Drift [°]	Mean [°]	Drift [°]	Mean [km/s]	Drift [km/s]
IMO 2012	340	338–343	243.7	+0.9	+43.0	+0.0	40.8	—

4 February η-Draconids

To improve the outcome a bit, we searched additionally for showers with an activity interval shorter than five degrees. This yielded the February η-Draconids (427 FED), which can be detected between February 3 and 6, when they are briefly the second strongest source in the sky. About 150 meteor from our database are assigned to that shower, which shows only little scatter in its parameters. Our values are a good fit to the MDC data, although the velocity deviates a bit more (Table 3).

5 New shower candidate

There is only one candidate for a new meteor shower in February. We could assign to this candidate 180 meteors between February 27 and March 4. It reaches a rank of four to five, which is quite good. There is remarkable scatter in the shower parameters and no clear activity profile, which is why we consider it currently to be only a meteor shower hypothesis until there is independent confirmation (Table 4).

6 Other showers

Last but not least, there are traces of the π-Hydrids (101 PIH) in our February data, but the data set is not sufficient for an unquestionable detection of the shower. The February μ-Virginids (516 FMV) are found in only two solar longitude intervals, so this detection is also questionable.

References

Molau S. (2012). “Million meteors in the IMO Video Meteor Database”. `http://www.imonet.org/showers/` .

Molau S., Kac J., Berko E., Crivello S., Stomeo E., Igaz A., and Barentsen G. (2012). “Results of the IMO Video Meteor Network – February 2012”. *WGN, Journal of the IMO*, **40:3**, 101–107.

Handling Editor: Javor Kac

Table 5 – Observers contributing to 2013 February data of the IMO Video Meteor Network. Eff.CA designates the effective collection area.

Code	Name	Place	Camera	FOV [°2]	Stellar LM [mag]	Eff.CA [km2]	Nights	Time [h]	Meteors
BANPE	Bánfalvi	Zalaegerszeg/HU	Huvcse01 (0.95/5)	2423	3.4	361	3	18.3	15
BASLU	Bastiaens	Hove/BE	Urania1 (0.8/3.8)*	4545	2.5	237	4	19.5	14
BERER	Berkó	Ludányhalászi/HU	Hulud1 (0.8/3.8)	5542	4.8	3847	4	34.2	126
			Hulud2 (0.95/4)	3398	3.8	671	5	35.6	39
			Hulud3 (0.95/4)	4357	3.8	876	4	34.4	33
BIRSZ	Biro	Agostyán/HU	Huago (0.75/4.5)	2427	4.4	1036	8	44.3	45
BOMMA	Bombardini	Faenza/IT	Mario (1.2/4.0)	5794	3.3	739	12	21.4	149
BREMA	Breukers	Hengelo/NL	Mbb3 (0.75/6)	2399	4.2	699	9	46.5	74
			Mbb4 (0.8/8)	1470	5.1	1208	14	72.0	74
BRIBE	Brinkmann	Herne/DE	Hermine (0.8/6)	2374	4.2	678	14	72.6	101
		Bergisch Gladbach/DE	Klemoi (0.8/6)	2286	4.6	1080	13	71.2	92
CASFL	Castellani	Monte Baldo/IT	Bmh1 (0.8/6)	2350	5.0	1611	14	130.7	217
			Bmh2 (1.5/4.5)*	4243	3.0	371	12	114.1	169
CRIST	Crivello	Valbrevenna/IT	Bilbo (0.8/3.8)	5458	4.2	1772	18	163.7	407
			C3P8 (0.8/3.8)	5455	4.2	1586	21	156.6	268
			Stg38 (0.8/3.8)	5614	4.4	2007	18	171.6	425
CSISZ	Csizmadia	Baja/HU	Huvcse02 (0.95/5)	1606	3.8	390	10	11.4	28
ELTMA	Eltri	Venezia/IT	Met38 (0.8/3.8)	5631	4.3	2151	17	151.1	300
GONRU	Goncalves	Tomar/PT	Templar1 (0.8/6)	2179	5.3	1842	15	153.5	431
			Templar2 (0.8/6)	2080	5.0	1508	19	176.9	378
			Templar3 (0.8/8)	1438	4.3	571	22	180.8	296
			Templar4 (0.8/3.8)	4475	3.0	442	19	168.8	302
GOVMI	Govedič	Središče ob Dravi/SI	Orion3 (0.95/5)	2665	4.9	2069	6	27.8	38
			Orion4 (0.95/5)	2662	4.3	1043	3	18.9	25
IGAAN	Igaz	Baja/HU	Hubaj (0.8/3.8)	5552	2.8	403	11	42.9	58
		Debrecen/HU	Hudeb (0.8/3.8)	5522	3.2	620	16	66.9	115
		Budapest/HU	Hupol (1.2/4)	3790	3.3	475	6	38.1	12
JONKA	Jonas	Budapest/HU	Husor (0.95/4)	2286	3.9	445	6	50.7	42
KACJA	Kac	Ljubljana/SI	Orion1 (0.8/8)	1402	3.8	331	4	20.7	11
		Kamnik/SI	Cvetka (0.8/3.8)	4914	4.3	1842	6	34.5	73
			Rezika (0.8/6)	2270	4.4	840	4	29.9	110
			Stefka (0.8/3.8)	5471	2.8	379	5	31.7	77
KOSDE	Koschny	Izana Obs./ES	Icc7 (0.85/25)*	714	5.9	1464	19	138.4	818
		Noordwijkerhout/NL	Lic4 (1.4/50)*	2027	6.0	4509	9	55.2	74

Table 5 – Observers contributing to 2013 February data of the IMO Video Meteor Network – continued from previous page.

Code	Name	Place	Camera	FOV [°2]	Stellar LM [mag]	Eff.CA [km^2]	Nights	Time [h]	Meteors
LERAR	Leroy	Gretz/FR	Saphira (1.2/6)	3260	3.4	301	10	58.3	28
MACMA	Maciejewski	Chelm/PL	Pav35 (1.2/4)	4383	2.5	253	7	20.5	24
			Pav36 (1.2/4)*	5732	2.2	227	7	22.2	41
			Pav43 (0.95/3.75)*	2544	2.7	176	4	18.4	13
MARGR	Maravelias	Lofoupoli-Crete/GR	Loomecon (0.8/12)	738	6.3	2698	14	76.1	165
MOLSI	Molau	Seysdorf/DE	Avis2 (1.4/50)*	1230	6.9	6152	2	20.4	155
			Mincam1 (0.8/8)	1477	4.9	1084	9	42.5	72
		Ketzür/DE	Remo1 (0.8/8)	1467	5.9	2837	13	76.5	321
			Remo2 (0.8/8)	1478	6.3	4467	12	67.7	259
			Remo3 (0.8/8)	1420	5.6	1967	8	59.2	68
MORJO	Morvai	Fülöpszállás/HU	Huful (1.4/5)	2522	3.5	532	10	49.0	34
OCAFR	Ocaña González	Madrid/ES	Fogcam (1.4/7)	1890	3.9	109	21	160.2	136
OCHPA	Ochner	Albiano/IT	Albiano (1.2/4.5)	2944	3.5	358	11	11.5	73
OTTMI	Otte	Pearl City/US	Orie1 (1.4/5.7)	3837	3.8	460	12	65.3	170
PERZS	Perko	Becsehely/HU	Hubec (0.8/3.8)*	5498	2.9	460	10	50.5	147
PUCRC	Pucer	Nova vas nad Dragonjo/SI	Mobcam1 (0.75/6)	2398	5.3	2976	19	145.8	274
SARAN	Saraiva	Carnaxide/PT	Ro1 (0.75/6)	2362	3.7	381	21	167.4	227
			Ro2 (0.75/6)	2381	3.8	459	22	193.8	274
			Sofia (0.8/12)	738	5.3	907	21	173.6	203
SCALE	Scarpa	Alberoni/IT	Leo (1.2/4.5)*	4152	4.5	2052	13	77.7	104
SCHHA	Schremmer	Niederkrüchten/DE	Doraemon (0.8/3.8)	4900	3.0	409	17	85.9	138
SLAST	Slavec	Ljubljana/SI	Kayak1 (1.8/28)	563	6.2	1294	4	13.7	19
STOEN	Stomeo	Scorze/IT	Min38 (0.8/3.8)	5566	4.8	3270	20	130.6	461
			Noa38 (0.8/3.8)	5609	4.2	1911	15	116.0	314
			Sco38 (0.8/3.8)	5598	4.8	3306	19	133.7	455
STRJO	Strunk	Herford/DE	Mincam2 (0.8/6)	2362	4.6	1152	6	36.0	46
			Mincam3 (0.8/12)	728	5.7	975	8	44.5	42
			Mincam5 (0.8/6)	2349	5.0	1896	9	52.8	85
TEPIS	Tepliczky	Budapest/HU	Humob (0.8/6)	2388	4.8	1607	5	26.8	66
TRIMI	Triglav	Velenje/SI	Sraka (0.8/6)*	2222	4.0	546	8	12.0	60
YRJIL	Yrjölä	Kuusankoski/FI	Finexcam (0.8/6)	2337	5.5	3574	4	26.9	41
ZELZO	Zelko	Budapest/HU	Huvcse03 (1.0/4.5)	2224	4.4	933	2	13.9	17
						Overall	28	4 854.3	9 968

* active field of view smaller than video frame

Results of the IMO Video Meteor Network — March 2013

Sirko Molau[1], *Javor Kac*[2], *Erno Berko*[3], *Stefano Crivello*[4], *Enrico Stomeo*[5], *Antal Igaz*[6], *Geert Barentsen*[7] *and Rui Goncalves*[8]

In March 2013, 69 cameras of the IMO Video Meteor Network recorded more than 11 000 meteors in almost 5 900 hours of observing time. Shower parameters for the x-Herculids are presented. The Antihelion complex source is explored. Three segments of activity are identified, with two belonging to the η- and λ-Viginids, and the κ-Virginids. The third segment represents a possibly new meteor shower. Shower parameters are presented for all three segments.

Received 2013 May 22

1 Introduction

Continuing the slow start to the year 2013, the weather did not improve significantly in March. Only the distribution was a little different, as this time observers in southern Europe had to deal with particularly poor weather conditions, whereas it was still acceptable farther north. Overall we collected far less data than in 2012 (Molau et al., 2012). 11 000 recorded meteors and almost 5 900 hour of effective observing time are a reduction of roughly 40% compared to the results from the previous year (Table 6 and Figure 1). Only seven out of 69 active camera systems obtained data in twenty or more nights, which is even worse than in February, as there were more cameras and three more observing nights in March.

With Karl-Heinz Gansel from Dingden in Germany we gained another observer for our camera network. Karl-Heinz is an active radio meteor observer and has some experiences with UFOCapture. Now he operates another camera station in the western part of Germany. Daro01 consists of a Watec 902H2 with a 3.6 mm lens ($f/1.4$). Karl-Heinz plans to switch to a more powerful lens in the future.

As March does not present any larger meteor showers, we will now look directly at the results of the long-term analysis in spring 2012 (Molau, 2012) for this month.

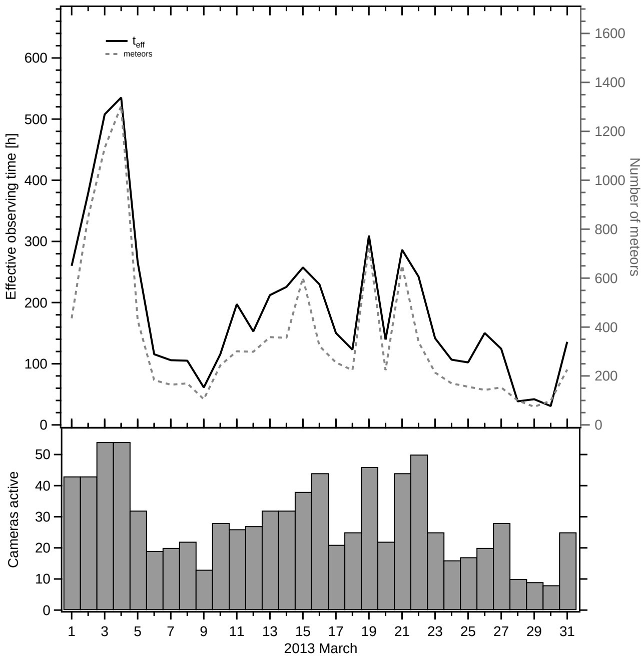

Figure 1 – Monthly summary for the effective observing time (solid black line), number of meteors (dashed gray line) and number of cameras active (bars) in 2013 March.

2 x-Herculids

The x Herculids (346 XHE) are active for a short time. Their activity interval spans only five degrees in solar longitude. However, between March 11 and 16 the Herculids are the strongest or second strongest source in the sky, which is why their detection is doubtless. Our shower parameters, which were derived from 300 meteors, show clear scatter in right ascension, but only little deviation in declination and velocity. There is a good agreement with the MDC list values (Table 1) which is no surprise given that we detected the shower on our own in 2009.

3 Antihelion complex

Between the end of February and mid-April there are a number of sub-radiants in Virgo which belong to the Antihelion complex. Over 2 000 meteors from our database could be assigned to these radiants. The scatter in the radiant parameters is typically quite large, but when the parameters are plotted over solar longitude (Figure 2), roughly three distinct segments can be identified in the data.

The first shower (red diamonds) lasts from late February until the first third of March, when it typically reaches a rank of about five. There is no significant drift in right ascension or declination, and the velocity is higher than for typical Virginid meteors.

[1]Abenstalstr. 13b, 84072 Seysdorf, Germany. Email: sirko@molau.de
[2]Na Ajdov hrib 24, 2310 Slovenska Bistrica, Slovenia. Email: javor.kac@orion-drustvo.si
[3]Bercsenyi ut 3, 3188 Ludanyhalaszi, Hungary. Email: berkoerno@invitel.hu
[4]Via Bobbio 9a/18, 16137 Genova, Italy. Email: stefano.crivello@libero.it
[5]via Umbria 21/d, 30037 Scorze (VE), Italy. Email: stom@iol.it
[6]Húr u. 9/D, H-1223 Budapest, Hungary. Email: antaligaz@yahoo.com
[7]University of Hertfordshire, Hatfield AL10 9AB, United Kingdom. Email: geert@barentsen.be
[8]Urbanizacao da Boavista, Lote 46, Linhaceira, 2305-114 Asseiceira, Tomar, Portugal. Email: rui.goncalves@ipt.pt

IMO bibcode WGN-413-molau-vidmar
NASA-ADS bibcode 2013JIMO...41...96M

Table 1 – Parameters of the x-Herculids from the MDC Working List and the analysis of the IMO Network in 2012.

Source	Solar Longitude		Right Ascension		Declination		v_∞	
	Mean [°]	Interval [°]	Mean [°]	Drift [°]	Mean [°]	Drift [°]	Mean [km/s]	Drift [km/s]
MDC	352	—	254	—	+48	—	36	—
IMO 2012	352	350–355	256.0	+0.8	+48.5	−0.0	36.8	—

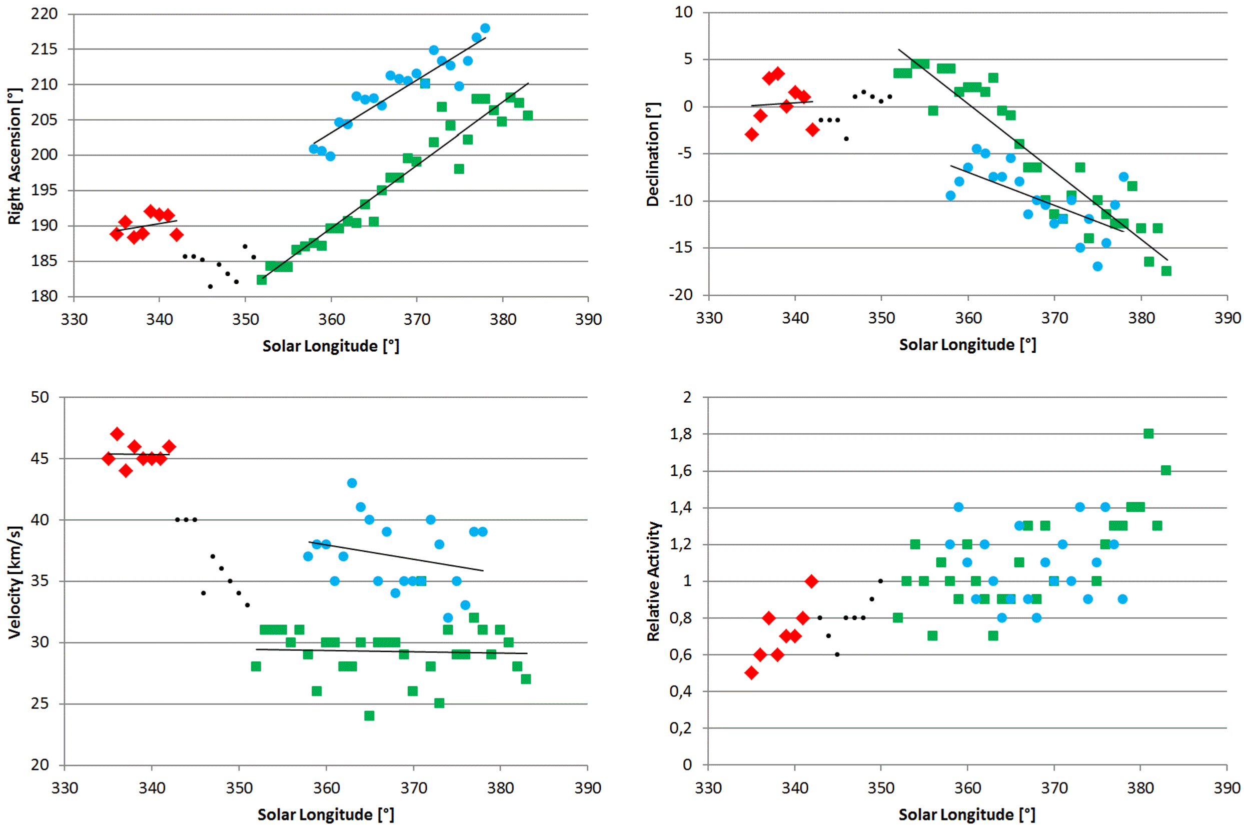

Figure 2 – Shower parameters for the radiants in the Virginid complex plotted over the solar longitude: Right ascension (upper left), declination (upper right), velocity (bottom left) and relative activity (bottom right).

The second segment (green squares) last from mid-March to mid-April. For most of the time it is the strongest meteor source in the sky. The right ascension is growing steadily, while the declination drops from +5° to −15°. The velocity is constant.

Between the first and second segment, there is a transition phase (small black dots), where the radiants have parameter values in-between segment one and two, and where the velocity is dropping by one km/s per day. This seems not plausible, which is why we omitted this transition phase.

Finally there is a third segment in the last third of March and first third of April (blue circles), which has typically a rank of three to four. Its drift in right ascension is similar to the second segment, but it is located more than ten degrees east. The declination is dropping as well, though at a smaller rate than the second segment, and the velocity is 7–8 km/s higher.

Matching these segments with meteor shower entries from the MDC list, we come up with the following result: The first shower does not match any of the list entries, particularly due to the large velocity (Table 2).

The second segment fits both to the η-Virginids (11 EVI) and λ-Virginids (49 LVI). The η-Virginids mark the begin of the activity interval and the λ-Virginids the end, so obviously these showers are identical (Table 3).

The third segment fits well to the κ-Virginids (509 KVI) (Table 4).

4 Possible new shower

Beyond the Virginid complex, there may be another unknown shower in our database, active between March 7 and 10. Overall we assigned almost 150 meteors to that shower candidate. There is only little scatter in the parameters and the radiant reaches a rank of six to seven. Since the activity interval is so short, we will wait for an independent confirmation of this shower candidate before it is formally reported to the MDC.

A quick look at the SonotaCo network database showed no clear concentration of orbits at the expected positions of the two shower candidates.

5 Other shower

Finally we found traces of the ζ-Serpentids (43 ZSE) in the March data, but the currently existing data set does not allow for an unequivocal identification of this shower.

Table 2 – Parameters of a possibly unknown meteor shower from the analysis of the IMO Network in 2012.

Source	Solar Longitude		Right Ascension		Declination		v_∞	
	Mean [°]	Interval [°]	Mean [°]	Drift [°]	Mean [°]	Drift [°]	Mean [km/s]	Drift [km/s]
IMO 2012	339	335–342	190	+0.2	+0	+0.1	45	—

Table 3 – Parameters of the η and λ-Virginids from the MDC Working List and the analysis of the IMO Network in 2012.

Source	Solar Longitude		Right Ascension		Declination		v_∞	
	Mean [°]	Interval [°]	Mean [°]	Drift [°]	Mean [°]	Drift [°]	Mean [km/s]	Drift [km/s]
MDC/EVI	354	—	182.1	+1	+2.6	−0.37	31.3	—
MDC/LVI	20	—	210.7	—	−10.2	—	29.0	—
IMO 2012	7	352–23	196	+0.9	−5	−0.7	29	—

Table 4 – Parameters of the κ-Virginids from the MDC Working List and the analysis of the IMO Network in 2012.

Source	Solar Longitude		Right Ascension		Declination		v_∞	
	Mean [°]	Interval [°]	Mean [°]	Drift [°]	Mean [°]	Drift [°]	Mean [km/s]	Drift [km/s]
MDC	6	—	208	+0.92	−8	−0.35	39	—
IMO 2012	9	358–18	210	+0.75	−10	−0.4	37	−0.1

Table 5 – Parameters of a possibly unknown meteor shower from the analysis of the IMO Network in 2012.

Source	Solar Longitude		Right Ascension		Declination		v_∞	
	Mean [°]	Interval [°]	Mean [°]	Drift [°]	Mean [°]	Drift [°]	Mean [km/s]	Drift [km/s]
IMO 2012	347	346–349	233	+0.6	+43	+0.0	42	—

References

Molau S. (2012). "Million meteors in the IMO Video Meteor Database". `http://www.imonet.org/showers/` .

Molau S., Kac J., Berko E., Crivello S., Stomeo E., Igaz A., and Barentsen G. (2012). "Results of the IMO Video Meteor Network – March 2012". *WGN, Journal of the IMO*, **40:3**, 108–112.

Handling Editor: Javor Kac

Code	Name	Place	Camera	FOV [°²]	Stellar LM [mag]	Eff.CA [km²]	Nights	Time [h]	Meteors
ARLRA	Arlt	Ludwigsfelde/DE	Ludwig1 (0.8/8)	1488	4.8	726	9	70.8	57
BANPE	Bánfalvi	Zalaegerszeg/HU	Huvcse01 (0.95/5)	2423	3.4	361	10	81.0	96
BASLU	Bastiaens	Hove/BE	Urania1 (0.8/3.8)*	4545	2.5	237	5	39.6	19
BERER	Berkó	Ludányhalászi/HU	Hulud1 (0.8/3.8)	5542	4.8	3847	9	64.8	224
			Hulud2 (0.95/4)	3398	3.8	671	8	61.7	70
			Hulud3 (0.95/4)	4357	3.8	876	8	63.5	78
BIRSZ	Biro	Agostyán/HU	Huago (0.75/4.5)	2427	4.4	1036	15	105.4	127
BOMMA	Bombardini	Faenza/IT	Mario (1.2/4.0)	5794	3.3	739	9	19.4	144
BREMA	Breukers	Hengelo/NL	Mbb3 (0.75/6)	2399	4.2	699	11	69.5	91
			Mbb4 (0.8/8)	1470	5.1	1208	16	98.9	89
BRIBE	Brinkmann	Herne/DE	Hermine (0.8/6)	2374	4.2	678	18	100.7	133
		Bergisch Gladbach/DE	Klemoi (0.8/6)	2286	4.6	1080	18	114.9	135
CASFL	Castellani	Monte Baldo/IT	Bmh1 (0.8/6)	2350	5.0	1611	13	93.7	198
			Bmh2 (1.5/4.5)*	4243	3.0	371	9	90.1	139
CRIST	Crivello	Valbrevenna/IT	Bilbo (0.8/3.8)	5458	4.2	1772	20	104.0	218
			C3P8 (0.8/3.8)	5455	4.2	1586	17	114.5	175
			Stg38 (0.8/3.8)	5614	4.4	2007	23	133.1	297
ELTMA	Eltri	Venezia/IT	Met38 (0.8/3.8)	5631	4.3	2151	9	71.9	129
GANKA	Gansel	Dingden/DE	Daro01 (1.4/3.6)	7141	3.1	652	4	25.3	13
GONRU	Goncalves	Tomar/PT	Templar1 (0.8/6)	2179	5.3	1842	9	58.7	148
			Templar2 (0.8/6)	2080	5.0	1508	15	89.8	174
			Templar3 (0.8/8)	1438	4.3	571	17	102.6	117
			Templar4 (0.8/3.8)	4475	3.0	442	14	73.3	147
GOVMI	Govedič	Središče ob Dravi/SI	Orion3 (0.95/5)	2665	4.9	2069	13	85.2	115
			Orion4 (0.95/5)	2662	4.3	1043	14	103.1	132
IGAAN	Igaz	Baja/HU	Hubaj (0.8/3.8)	5552	2.8	403	19	88.8	80
		Debrecen/HU	Hudeb (0.8/3.8)	5522	3.2	620	13	93.3	146
		Budapest/HU	Hupol (1.2/4)	3790	3.3	475	9	74.8	30
JONKA	Jonas	Budapest/HU	Husor (0.95/4)	2286	3.9	445	12	75.5	73
KACJA	Kac	Ljubljana/SI	Orion1 (0.8/8)	1402	3.8	331	9	73.4	39
		Kamnik/SI	Cvetka (0.8/3.8)	4914	4.3	1842	10	78.9	232
			Rezika (0.8/6)	2270	4.4	840	10	79.8	353
			Stefka (0.8/3.8)	5471	2.8	379	9	76.5	189
KISSZ	Kiss	Sülysáp/HU	Husul (0.95/5)*	4295	3.0	355	10	76.7	28
KOSDE	Koschny	Izana Obs./ES	Icc7 (0.85/25)*	714	5.9	1464	21	166.3	856
		Noordwijkerhout/NL	Lic4 (1.4/50)*	2027	6.0	4509	13	73.4	115

Table 6 – Observers contributing to 2013 March data of the IMO Video Meteor Network. Eff.CA designates the effective collection area.

Table 6 – Observers contributing to 2013 March data of the IMO Video Meteor Network – continued from previous page.

Code	Name	Place	Camera	FOV [°²]	Stellar LM [mag]	Eff.CA [km²]	Nights	Time [h]	Meteors
LERAR	Leroy	Gretz/FR	Saphira (1.2/6)	3260	3.4	301	14	71.7	33
MACMA	Maciejewski	Chelm/PL	Pav35 (1.2/4)	4383	2.5	253	13	76.0	73
			Pav36 (1.2/4)*	5732	2.2	227	11	88.8	127
			Pav43 (0.95/3.75)*	2544	2.7	176	11	96.1	56
MARGR	Maravelias	Lofoupoli-Crete/GR	Loomecon (0.8/12)	738	6.3	2698	20	89.3	142
MOLSI	Molau	Seysdorf/DE	Avis2 (1.4/50)*	1230	6.9	6152	13	83.8	651
			Mincam1 (0.8/8)	1477	4.9	1084	18	124.2	138
		Ketzür/DE	Remo1 (0.8/8)	1467	5.9	2837	21	154.1	570
			Remo2 (0.8/8)	1478	6.3	4467	21	149.4	488
			Remo3 (0.8/8)	1420	5.6	1967	18	146.0	107
MORJO	Morvai	Fülöpszállás/HU	Huful (1.4/5)	2522	3.5	532	16	108.5	82
OCAFR	Ocaña González	Madrid/ES	Fogcam (1.4/7)	1890	3.9	109	17	105.2	84
OCHPA	Ochner	Albiano/IT	Albiano (1.2/4.5)	2944	3.5	358	1	0.7	4
OTTMI	Otte	Pearl City/US	Orie1 (1.4/5.7)	3837	3.8	460	19	96.5	193
PERZS	Perko	Becsehely/HU	Hubec (0.8/3.8)*	5498	2.9	460	16	116.8	355
PUCRC	Pucer	Nova vas nad Dragonjo/SI	Mobcam1 (0.75/6)	2398	5.3	2976	15	105.9	198
ROTEC	Rothenberg	Berlin/DE	Armefa (0.8/6)	2366	4.5	911	8	76.0	93
SARAN	Saraiva	Carnaxide/PT	Ro1 (0.75/6)	2362	3.7	381	12	50.0	77
			Ro2 (0.75/6)	2381	3.8	459	11	52.2	71
			Sofia (0.8/12)	738	5.3	907	11	56.0	58
SCALE	Scarpa	Alberoni/IT	Leo (1.2/4.5)*	4152	4.5	2052	5	30.5	55
SCHHA	Schremmer	Niederkrüchten/DE	Doraemon (0.8/3.8)	4900	3.0	409	16	102.4	165
SLAST	Slavec	Ljubljana/SI	Kayak1 (1.8/28)	563	6.2	1294	4	20.7	39
STOEN	Stomeo	Scorze/IT	Min38 (0.8/3.8)	5566	4.8	3270	13	74.4	247
			Noa38 (0.8/3.8)	5609	4.2	1911	11	75.4	226
			Sco38 (0.8/3.8)	5598	4.8	3306	11	70.7	234
STRJO	Strunk	Herford/DE	Mincam2 (0.8/6)	2362	4.6	1152	15	101.4	116
			Mincam3 (0.8/12)	728	5.7	975	16	120.6	127
			Mincam4 (1.0/2.6)	9791	2.7	552	1	8.0	5
			Mincam5 (0.8/6)	2349	5.0	1896	17	118.1	170
TEPIS	Tepliczky	Budapest/HU	Humob (0.8/6)	2388	4.8	1607	11	84.6	162
TRIMI	Triglav	Velenje/SI	Sraka (0.8/6)*	2222	4.0	546	15	17.9	114
YRJIL	Yrjölä	Kuusankoski/FI	Finexcam (0.8/6)	2337	5.5	3574	24	185.6	346
						Overall	31	5 850.4	11 012

* active field of view smaller than video frame

The International Meteor Organization

web site http://www.imo.net

Council

President: Jürgen Rendtel,
Eschenweg 16, D-14476 Marquardt, Germany.
tel. +49 33208 50753
e-mail: jrendtel@aip.de

Vice-President Cis Verbeeck,
Bogaertsheide 5, 2560 Kessel, Belgium.
e-mail: cis.verbeeck@scarlet.be

Secretary-General: Robert Lunsford
1828 Cobblecreek Street, Chula Vista,
CA 91913-3917, USA. tel. +1 619 585 9642
e-mail: lunro.imo.usa@cox.net

Treasurer: Marc Gyssens, Heerbaan 74,
B-2530 Boechout, Belgium.
e-mail: marc.gyssens@uhasselt.be
BIC: GEBABEBB
IBAN: BE30 0014 7327 5911
Always state BIC and IBAN codes together!
Check international transfer charges with your bank; you are responsible for paying these.

Other Council members:
Rainer Arlt, Bahnstr. 11, D-14974 Ludwigsfelde, Germany. e-mail: rarlt@aip.de
David Asher, Armagh Observatory, College Hill, Armagh, Northern Ireland BT61 9DG, UK. e-mail: dja@arm.ac.uk
Geert Barentsen, University of Hertfordshire, Hatfield AL10 9AB, UK. e-mail: geert@barentsen.be
Javor Kac (see details under WGN)
Detlef Koschny, Zeestraat 46, NL-2211 XH Noordwijkerhout, Netherlands. e-mail: detlef.koschny@esa.int
Sirko Molau, Abenstalstraße 13b, D-84072 Seysdorf, Germany. e-mail: sirko@molau.de
Paul Roggemans (see details under IMC Liaison Officer)

Commission Directors

FIreball DAta Center: André Knöfel
Am Observatorium 2,
D-15848 Lindenberg, Germany.
e-mail: fidac@imo.net
Photographic Commission: vacant
Radio Commission: Jean-Louis Rault
Société Astronomique de France,
16, rue de la Vallée,
91360 Epinay sur Orge, France.
email: f6agr@orange.fr
Telescopic Commission: Malcolm Currie
660, N'Aohoku Place, Hilo, HI 96720, USA
e-mail: mjc@star.rl.ac.uk
Video Commission: Sirko Molau
Visual Commission: Rainer Arlt

IMC Liaison Officer

Paul Roggemans, Pijnboomstraat 25, 2800 Mechelen, Belgium, email: paul.roggemans@gmail.com

WGN

Editor-in-chief: Javor Kac
Na Ajdov hrib 24, SI-2310 Slovenska Bistrica, Slovenia. e-mail: wgn@imo.net;
include METEOR in the e-mail subject line

IMO Sales

Available from the Treasurer or the Electronic Shop on the IMO Website	€	$
IMO membership, including subscription to WGN Vol. 41 (2013)		
Surface mail	26	39
Air Mail (outside Europe only)	49	69
Electronic subscription only	21	29
Back issues of WGN on paper (price per complete volume)		
Vols. 26 (1998) – 35 (2007) except 30 (2002), 38 (2010) – 40 (2012)	15	23
Vols. 37 (2009) – 40 (2012) – electronic version only	9	13
Proceedings of the International Meteor Conference on paper		
1990, 1991, 1993, 1995, 1996, 1999, 2000, 2002, 2003, per year	9	13
2007, 2009, 2010, 2011	15	23
Proceedings of the Meteor Orbit Determination Workshop 2006	15	23
Proceedings of the Radio Meteor School 2005 on paper	15	23
Handbook for Meteor Observers	20	29
Electronic media		
Meteor Beliefs Project CD-ROM	5	7
DVD: WGN Vols. 6–30 & IMC 1991, 1993–96, 2001–04	45	69

2012 video meteors from Hungary

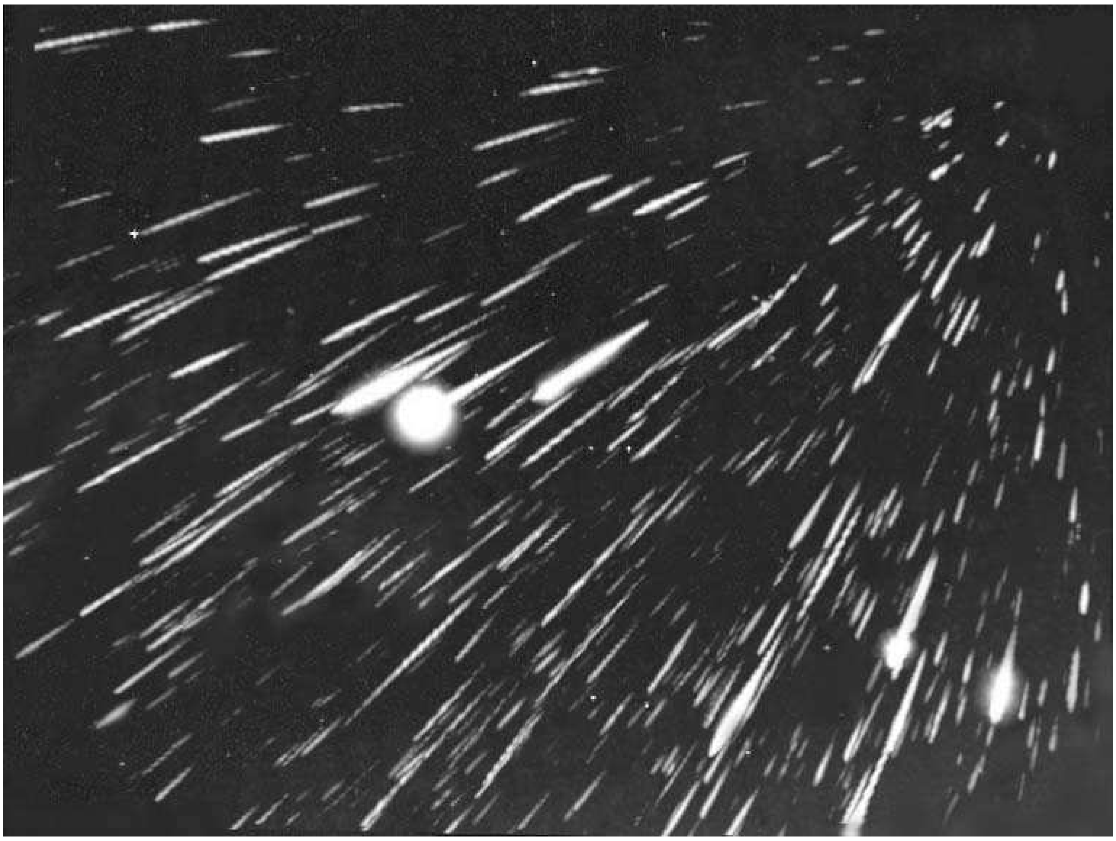

Composite image of 720 Perseid meteors, recorded between 2012 August 7 and 15 by the HULUD1 camera, equipped with 3.8 mm Computar lens. Image courtesy of Erno Berkó.

Composite image of 315 Geminid meteors, captured on 2012 December 12/13 by the HULUD1 camera, equipped with 3.8 mm Computar lens. Image courtesy of Erno Berkó.